SC-14-0541.Accepted

# PRMT1 and PRMT8 regulate retinoic acid dependent neuronal differentiation with implications to neuropathology

Zoltan Simandi[1], Erik Czipa[1], Attila Horvath[1], Aron Koszeghy[2], Csilla Bordas[2], Szilárd Póliska[1], István Juhász[3,4], László Imre[5], Gábor Szabó[5], Balazs Dezso[6], Endre Barta[1], Sascha Sauer[7], Katalin Karolyi[8], Ilona Kovacs[8], Gábor Hutóczky[9], László Bognár[9], Álmos Klekner[9], Peter Szucs[2,10], Bálint L.Bálint[1] and Laszlo Nagy[1,11,12#]

[1]Department of Biochemistry and Molecular Biology, University of Debrecen, Debrecen, Hungary, H-4012

[2]Department of Physiology, University of Debrecen, Debrecen, Hungary, H-4012

[3]Department of Dermatology, University of Debrecen, Debrecen, Hungary, H-4012

[4]Department of Surgery and Operative Techniques, Faculty of Dentistry, University of Debrecen, Debrecen, Hungary, H-4012

[5]Department of Biophysics and Cell biology, University of Debrecen, Debrecen, Hungary, H-4012

[6]Department of Pathology, University of Debrecen, Debrecen, Hungary, H-4012

[7]Otto Warburg Laboratory, Max Planck Institute for Molecular Genetics, Berlin, Germany

[8]Department of Pathology, Kenézy Hospital and Outpatient Clinic, Bartok Bela 2-26, Debrecen, Hungary, H-4010

[9]Department of Neurosurgery, University of Debrecen, Debrecen, Hungary, H-4012

[10]MTA-DE-NAP B-Pain Control Group, University of Debrecen, Debrecen, Hungary, H-4012

[11]MTA-DE "Lendulet" Immunogenomics Research Group, University of Debrecen, Debrecen, Hungary, H-4012

[12]Sanford-Burnham Medical Research Institute at Lake Nona, 6400 Sanger Road, Orlando FL 32827, USA

[#]**Correspondence information:**

Name: Laszlo Nagy

Address: 6400 Sanger Road, Orlando, FL 32827

Phone: +1-407-745-2150

e-mail: lnagy@sanfordburnham.org

**Running title**

PRMT1 and PRMT8 regulate neural cell specification

**Author contribution summary**

Zoltan Simandi: Conception and design, Collection and/or assembly of data, Data analysis and interpretation, Manuscript writing

Erik Czipa: Data analysis and interpretation

Attila Horvath: Data analysis and interpretation

Aron Koszeghy: Collection and/or assembly of data, Data analysis and interpretation

Csilla Bordas: Collection and/or assembly of data

Szilárd Póliska: Collection and/or assembly of data

István Juhász: Provision of study material

László Imre: Collection and/or assembly of data

Gábor Szabó: Collection and/or assembly of data

Balazs Dezso: Data analysis and interpretation

Endre Barta: Data analysis and interpretation

Sascha Sauer: Collection and/or assembly of data

Katalin Karolyi: Collection and/or assembly of data

Ilona Kovacs: Collection and/or assembly of data

Gábor Hutóczky: Collection and/or assembly of data

László Bognár: Collection and/or assembly of data

Álmos Klekner: Collection and/or assembly of data

Péter Szűcs: Data analysis and interpretation

Bálint L.Bálint: Financial support, Conception and design, Data analysis and interpretation

László Nagy: Conception and design, Data analysis and interpretation, Financial support, Manuscript writing, Final approval of manuscript

**Key words**

PRMT1, PRMT8, retinoid signaling, neural differentiation, glioblastoma

**Highlights**

- PRMT1 is a selective repressor of early retinoid response in ESCs
- PRMT8 is a direct retinoid target gene
- PRMT8 is a co-activator of retinoid response in differentiating neurons
- PRMT1 and PRMT8 collaborate and regulate neuron cell type specification
- PRMT1 and PRMT8 affects functions of terminally differentiated neurons
- Human glioblastoma tissues lack PRMT8 expression

**Abstract**

Retinoids are morphogens and have been implicated in cell fate commitment of embryonic stem cells (ESCs) to neurons. Their effects are mediated by RAR and RXR nuclear receptors. However, transcriptional co-factors required for cell and gene-specific retinoid signaling are not known. Here we show that Protein aRginine Methyl Transferase (PRMT) 1 and 8 have key roles in determining retinoid regulated gene expression and cellular specification in a multistage neuronal differentiation of murine ESCs. PRMT1 acts as a selective modulator, providing the cells with a mechanism to reduce the potency of retinoid signals on regulatory "hotspots". PRMT8 is a retinoid receptor target gene itself and acts as a cell type specific transcriptional co-activator of retinoid signaling at later stages of differentiation. Lack of either of them leads to reduced nuclear arginine methylation, dysregulated neuronal gene expression and altered neuronal activity. Importantly, depletion of PRMT8 results in altered expression of a distinct set of genes, including markers of gliomagenesis. PRMT8 is almost entirely absent in human glioblastoma tissues. We propose that PRMT1 and PRMT8 serve as a rheostat of retinoid signaling to determine neuronal cell specification in a context-dependent manner, and might also be relevant in the development of human brain malignancy.

## 1. Introduction

Animal cells in developing embryos receive positional signals from diffusible molecules, called morphogens. Retinoic acid (RA), a natural metabolite of vitamin A, has been proposed to be a vertebrate morphogen [1, 2]. Molecularly, RA acts via the activation of RAR:RXR heterodimers. RARs and RXRs are two subfamilies of nuclear receptors (NRs) that bind to DNA motifs called RA-response elements (RAREs), typically arranged as direct repeats (DR), and regulate transcription [3]. Unliganded RAR:RXR heterodimers bind to co-repressor complexes and are thought to maintain target genes in a repressed state [4]. Ligand binding stimulates a cascade of events resulting in the release of the co-repressor complexes, recruitment of transcriptional co-activators and thus initiation of transcription [5, 6]. However, the composition of co-activator and co-repressor complexes is cell-type and context dependent and contributes to cell specification and potentially gene-specific transcription [7].

Members of the Protein aRginineMethyltransferase (PRMT) family have been shown to act as nuclear receptor co-activators [8-11]. Based on their enzyme activity PRMTs are grouped into three groups. Type I enzymes (PRMT1, 2, 3, 4, 6 and 8) catalyze the formation of asymmetric dimethylarginine (aDMA) residues while the Type II (PRMT5) enzyme catalyze the formation of symmetric dimethylarginine (sDMA) residues. Both Type I and II enzymes generate monomethylarginine (MMA) intermediates. The Type III enzyme (PRMT7) only generates a MMA mark [12].

Importantly, asymmetric arginine methylation is associated with cellular differentiation [13, 14]. Early studies revealed high level of aDMA in the nervous system [15], however expression profile of Type I PRMTs and their functional contribution to neurogenesis remained largely uncharacterized [16-19].

PRMT1 is a major type of protein arginine methyltransferase and the most studied one [20]. Importantly, PRMT1 null mice die at an early stage, indicating its essential role in embryonic development [17]. PRMT1-dependent methylation of Arg3 on H4 tail peptides facilitates P300-mediated histone H4 acetylation *in vitro* [21-23]. These studies collectively suggest that PRMT1 is likely to collaborate with P300 to regulate transcription.

Mechanistically, PRMT1 dimerization/oligomerization or heterodimerization may be required for PRMT1 to achieve its co-activator function [24]. A comparison of mammalian PRMTs revealed that PRMT8 is PRMT1's closest paralogue within this enzyme family, with an identical exon structure and a brain specific expression pattern and can form a heterodimer with PRMT1 [25].

In this work, we explored the mechanistic and functional role of PRMT1 and PRMT8 using a multistage differentiation model of mouse embryonic stem cells (ESCs) to neurons. Our findings implicate asymmetric arginine methylation as a novel way to regulate the potency of retinoic acid regulated transcriptional response. We show that PRMT1 and PRMT8 are linked and act as part of a rheostat to integrate retinoid signaling into neuronal specific gene expression governed by retinoids with implications to neurological disorders.

## 2. Materials and methods

Additional details about all of the mehods listed below, information about the antibodies used and related citations can be found in the Supporting Information/Extended Experimental Procedures.

**mESC cultureand neural differentiation**

Wild type and genetically modified (see in the text) mouse ESCs (kind gift of Tomo Saric and Istvan Szatmari) were cultured on 0.1% gelatin coated plates in feeder-free condition in 5% $CO_2$ at 37˚C. Cells were differentiated through embryoid body formation [26].

**Ligands and treatment**

Cells were treated with vehicle (dimethylsulfoxide) or with the following ligands: LG268 (a gift from R. Heyman; Ligand Pharmaceuticals, San Diego, CA), RA (Sigma) or AM580 [27].

**Gene silencing assays**

shRNA lentiviral plasmids (MISSION shRNA, TRCN0000018490-493 and TRCN0000097479-482) were purchased from Sigma for targeting the mouse PRMT1 and PRMT8, respectively.

**Chromosome counting**

Cells were treated with colcemid (Sigma) for mitotic arrest and harvested by standard hypotonic treatment and methanol: acetic acid (3:1) fixation. Slides were prepared by standard air-drying method. Twenty DAPI stained chromosomal spreads were counted in each case.

**Teratoma assay**

Mouse ESCs were trypsinized and resuspended in 0.9% normal saline at a concentration of $5x10^6$ cells ml-1. SCID mice were anesthetized, and 100 μl of the cell suspension was injected into the lower leg. After 4~6 weeks, the teratomas were surgically dissected, fixed, embedded in paraffin and sectioned. The sections were then hematoxylin and eosin stained.

**Real-time quantitative RT-PCR**

Total RNA was isolated with TRIZOL reagent (Invitrogen). cDNA synthesis was performed with High Capacity cDNA Reverse Trancription kit (Applied Biosystems) according to the manufacturer's recommendation. Quantitative PCR was performed using real-time PCR (ABI PRISM 7900, Applied Biosystems). Gene expression was quantified by the comparative $C_T$ method and normalized to Gapdh. Values are expressed as mean ± SD of the mean. GraphPad Prism version 5.02 was used for data interpretation. The sequences of the primers and probes are available upon request.

**Calcium imaging, loose-patch and whole-cell patch-clamp recording**

ESCs were differentiated to neurons for 16 days. Whole cell patch clamp and calcium imaging

experiments were conducted on these cells to investigate their functional properties. For the measurement of intracellular calcium concentration changes, cells were and loaded with the calcium indicator dye Oregon Green 488 BAPTA-1, AM. Calcium imaging measurements has been was carried out as described by Koszeghy et al [28] with minor modifications. Patch clamp experiments were conducted similarly as in Koszeghy et al [28] with some alterations.

**RNA-seq and analysis**

RNA-Seq library was prepared from two biological replicates by using TruSeq RNA Sample Preparation Kit (Illumina) according to manufacturer protocol. Illumina RNA-sequencing was performed using standard procedures at the Centre National de Genotypage (CNG) Paris, France. The TopHat-Cufflinks-CummeRbund toolkit trio was used for mapping spliced reads, making transcript assemblies, and getting, sorting and visualizing gene expression data. Series accession number: SRP042072 / PRJNA248061.

**Microarray analysis**

Data has been analyzed using GeneSpring v12.6. All microarray data from this study have been submitted to the Gene Expression Omnibus (Series accession number: GSE37060 and GSE37060).

Genelists were imported into IPA (Ingenuity® Systems, www.ingenuity.com) to carry out pathway analysis.

**Enrichment of histone modification**

Cells were washed and labeled with rabbit anti-H4R3me2a primary antibody diluted 800× in 1% BSA / 1×PBS / 5mM EDTA at 4ºC overnight using a total volume of 150 µl labeling solution on each slides. Data evaluation and hardware control was performed by the iCys 3.4 software for Windows XP.

**Chromatin immunoprecipitation (ChIP) and sequencing**

ChIP-qPCR and ChIP-seq experiments were carried out as previously described [29], with minor modifications. Primary analysis of the ChIP-seq raw reads has been carried out using the ChIP-seq analyze command line pipeline. IGV was used for data visualization.

All ChIP-seq data from this study have been submitted to the Sequence Read Archive (SRA), NCBI (Series accession number: SRP042072 / PRJNA248061).

**Tissue samples**

Glioblastoma and normal brain tissues were collected during neurosurgical operations in the Department of Neurosurgery, University of Debrecen. Normal samples were collected either during functional neurosurgery for epilepsy or non-tumor herniated brain tissue during tumor surgery. Sections for histological analysis were cut from the same samples used for mRNA analysis. All procedures were approved by the National Ethical Committee, and every patient signed an informed consent form.

## 3. Results

**Asymmetric arginine methylation is present in distinct stages of retinoic acid induced neural differentiation**

To explore the involvment of arginine methylation in neuronal development, we set up an embryonic stem cell-based model system (Fig.1A). The four stages are: (I) undifferentiated embryonic stem cells, (II) aggregates of spontaneously differentiating cells (termed embryoid bodies (EBs)) (III) cells commited to neuroectoderm as a result of all-trans retinoic acid (RA) treatment and (IV) the fully differentiated neuronal cells [26]. Importantly, these terminally differentiated neurons have electrophysiological properties similar to those brain-derived neurons and show positive staining for synapsin (Fig.1B, Supporting Information Fig.S1A), this is in line with the findings of others on ESC derived neurons differentiated using the same method [30].

This model system allows a systematic step-by-step analysis of early cell fate commitment as well as late neural cell type specification. As Supporting Information Fig.S1B shows these stages can be characterized by distinct gene expression signatures. Undifferentiated ESCs express high level of stem cell specific Oct3/4 [31], while upon induction of spontaneous differentiation the level of Oct3/4 is declining. Treatment with RA causes the activation of retinoic acid signaling as it is reflected by the increased Rarβ expression. At this stage cells become Pax6-positive neural progenitor cells with the characteristics of radial glial cells [26]. Members of the Hox-family, such as Hoxb1, are also induced. In the last stage, high expression of Tuj1 and Dcx, two well established markers of neurogenesis can be detected [32].

Using this multistage differentiation system, we have found that proteins with symmetric and asymmetric dimethylated arginine (sDMA and aDMA) residues are present in ESCs (Fig.1C and Supporting Information Fig.S1C). Asymmetric arginine methylation level of these proteins was changing dynamically during retinoic acid induced neural differentiation, suggesting either an increased level of target proteins or overall Type I enzyme-activity. A 68 kDa protein (likely Sam68, a previously identified arginine methyltransferase target) [33] showed dramatically increased Asym24 level. Increased expression of Sam68 during neural differentiation could be also detected (Supporting Information Fig.S1C and S1D). Importantly, symmetric arginine methylation was not altered significantly (Fig.1C and Supporting Information Fig. S1C).

As the next step, we assessed the expression profile of PRMT-family members. Gene expression data obtained from RNA-seq in undifferentiated ESCs revealed the high level expression of PRMT1 in undifferentiated cells, suggesting its dominant role in ESCs arginine methylation (Fig.1D). RT-qPCR validation confirmed that PRMT1 is highly expressed in ESCs and its expression remained constant during neural differentiation showing a slight increase upon RA-

treatment (Fig.1E). Other Type I PRMTs, responsible for aDMA were less abundant in ESCs, but PRMT2, PRMT6 and PRMT8 showed significantly increased gene expression in differentiated neurons. In line with the unaltered sDMA level, expression of Type II PRMT5 was not changed (Fig.1E).

Importantly, we found that asymmetric arginine dimethylation of Histone 4 aRginine 3 (H4R3me2a) also indicated increased asymmetric arginine methylation upon differentiation (Fig.1F). H4R3me2a mark and the identified Sam68 methylation are deposited by PRMT1 and its closest paralogue PRMT8 [25, 34], however, their functional redundancy is not understood yet. These results drew our attention to the importance of PRMT1 and PRMT8 in neurogenesis. PRMT1 maintained a more or less even protein level during the course of RA-dependent neural differentiation, while PRMT8 was induced upon RA treatment and was present only in differentiated neurons (Fig.1G). H4R3me2a and PRMT8 showed nuclear localization, while PRMT1 could also be detected in the cytoplasm of differentiated neurons (Fig.1H).

**PRMT1 is responsible for arginine methylation in ESCs and affects transcription**

As a next step we established PRMT1 and PRMT8 knockdown ESCs to get functional insights into the role of these two proteins in neurogenesis. Although PRMT1 knockout ESCs were established previously [17], a proper genetic control was not available for comperative studies. Thus, we established PRMT1 and PRMT8 knockdown ESCs using shRNA based gene silencing (Fig.2A and 2B; Supporting Information Fig.S2A-S2F) in addition to PRMT1 knockout cells (Supporting Information Fig.S2G). Analysis of asymmetrically arginine dimethylated proteins using anti-ASYM24 antibody revealed hypomethylation of certain cellular proteins in PRMT1-depleted ESCs (Fig.2B, Supporting Information Fig.S2G). PRMT1 was mainly localized in the cytoplasmic fraction, however asymmetric arginine methylation was more abundant in the

nucleus (Fig.2C, Supporting Information Fig.S1C). ASYM24 decorated signal intensity decreased in both fractions as the result of PRMT1 silencing. The total amount of PRMT1 mediated H4R3me2a histone modification was also decreased (Fig.2D), further demonstrating the functional consequences of the loss of PRMT1 activity and indicating the role of PRMT1 in the regulation of chromatin. PRMT1-depleted or knockout cells showed typical ESC morphology and positive staining for well-established markers of pluripotency (Fig.2E, Supporting Information Fig.S2H).

To clarify the transcriptional consequences of the reduced level of PRMT1 in ESCs we carried out global transcriptional analyses using RNA-seq. Pathway analysis clarified that the 165 differentially expressed genes are mainly related to cellular movement (Hspb1, Fgfbp1, Ctgf, Cyr61), proliferation and p53-signaling (Camk2n1, Igfbp3, Smad7, Tpm1), tight junction and cytoskeletal elements (Myl9, Thbs1, Sepp1) (Fig.2F, Supporting Table 1). A role for PRMT1 in many of these cellular function has been previously suggested in other cellular model systems [35, 36]. Importantly, typical pluripotency markers were not affected by the loss of PRMT1, suggesting that PRMT1 in contrast to CARM1, is not required for the maintenance of pluripotency [14]. Importantly, 39 out of 165 significantly regulated genes showed upregulation in PRMT1 depleted ESCs vs. control cells, suggesting the loss of repression on these genes in hypomethylated cells (Fig.2F). Taken together, data obtained from gene-expression analysis indicate that PRMT1, beside its known transcriptional co-activator function, has a repressive feature on a set of genes, which might be relevant in various cellular functions.

Importance of arginine methylation of co-regulators was demonstrated by others [37, 38]. It has been also shown that methylation of Arg3 on H4 tail peptides facilitates P300-mediated histone acetylation *in vitro* [21-23]. In order to see whether P300 and PRMT1 are present in one complex in ESCs we carried out co-immunprecipitation experiments. Several asymmetrically arginine

methylated proteins were co-immunprecipitated by P300 but not with the isotope control (Fig.2G). Moreover, the asymmetric arginine methylation of these proteins were PRMT1-dependent.

To understand the contribution of PRMT1-mediated arginine methylation in P300-mediated transcriptional and epigenetic program of ESCs we determined the P300 cistrome in the presence and absence of PRMT1. We could identify 3420 consensus P300 binding sites present in both D3 and E14 control ESCs (see Supporting Information). Motif analysis revealed that P300 is mainly recruited to the stem cell specific transcription factor Oct3/4, Sox2, Klf4, Esrrb and Nanog (Fig.2H). Considering only those P300 bindings that were detectable and significant in both D3 and E14 cells between control and PRMT1-depleted cells we could identify only ~90 genomic regions. Half of these regions showed increased P300 occupancy in PRMT1 knockdowns (Fig.2I). We could identify only few examples where PRMT1-dependent P300 recruitment were coupled to differential gene expression (eg. Igsf21, Ankrd35, Sema3e, Colec12). These results suggest that, at least in undifferentiated ESCs, P300 occupancy is dominantly PRMT1-independent.

We next evaluated the differentiation potential of the PRMT1-depleted cells. Genome-wide comparison and RT-qPCR validation of spontaneously differentiated control and hypomethylated cells showed that classical lineage markers of endoderm, mesoderm and ectoderm were similarly induced upon spontaneous differentiation (Supporting Information Fig.S3A-S3C). Injection of PRMT1-/- ESCs into immunodeficient mice resulted in teratoma formation with obvious differentiated structures from all three germinal layers, excluding the possibility that residual PRMT1, present in knockdown cells, is sufficient for differentiation (Fig.2J). PRMT1-/- cells were also able to differentiate to Vimentin+ mesenchymal cells and TroponinC+ cardiomyocytes

(Supporting Information Fig.S3D), suggesting that cells can undergo differentiation to various cell types in the absence of PRMT1.

To identify differentiation-related signaling pathways that were affected in hypomethylated cells, we compared the gene expression profile at day 4 of differentiation. Pathway analysis based on altered expression of Dusp1, Fos, Smad3, Tgfb3, etc predicted RXR:LXR and RXR:RAR activation as one of the top canonical pathways being re-activated in the absence of PRMT1 (Fig.2K).

**PRMT1 selectively modulates the regulation retinoid target-genes**

Retinoic acid (RA), acting through the activation of RXR:RAR, is a general inducer of ESCs differentiation [39]. In order to characterize the early response of RA in PRMT1-depleted cells, we performed genome-wide comparison of gene expression in RA treated embryoid bodies (day 4). 12h RA treatment changed the expression of 127 genes in control cells and 492 genes in hypomethylated cells (Fig.3A). While most of the known retinoid targets, such as Cyp26a1, Dhrs3, Dleu7, Rbp1, Stra8 were induced to the same degree in PRMT1-depleted and control cells; Hoxa1, Hoxb1, Stra6, Pmp22 and Spsb1 also under retinoic acid control [40, 41], showed higher induction in hypomethylated cells (Fig.3B, Supporting Information Fig.S4 and S5A, S5B). Importantly, many genes (eg. Foxd3, Otx2) showed more pronounced RA-induced repression in PRMT1 knockdown cells, while Zfp428 and Fgf5 were only repressed in PRMT1-depleted cells (Fig.3B, Supporting Information Fig.S4). These results suggest a gene-selective regulatory effect of PRMT1 in the RA response of ESCs.

To further investigate this gene-selectivity at the promoter level, we transfected ESCs with the Hoxb1-promoter, containing the endogenous DR2 RA-response element, linked to a luciferase reporter gene [41] (Supporting Information Fig.S5C). Transient overexpression of PRMT1

resulted in a decrease in basal transcription level of Hoxb1 (Fig.3C). To a lesser extent Pmp22 and Spsb1 enhancers were also suppressed in the presence of PRMT1. The ligand induced retinoid response of Hoxb1 and Spsb1 were also decreased (Fig.3D). Accordingly, in the absence of PRMT1 RA-dependent transcriptional activity was markedly increased (Fig.3E). Importantly, PRMT1 had no effect in case of a synthetic canonical DR2 response element (Fig.3F), suggesting a context-dependent and promoter-selective effect of PRMT1 in the regulation of retinoid response.

P300 has been implicated as a regulator of retinoid response in F9 cells [42, 43]. In order to see, whether PRMT1-modulated, retinoic acid induced gene expression correlates with P300 binding, we first determined the RA-dependent P300 cistrome in ESCs. Upon RA treatment there was a ~3 fold reduction in the number of P300 binding sites in control cells (Fig.3G) and also the occupancy was substantially decreased (Fig.3H). We could observe similar P300 redistribution in the PRMT1 knockdown cells (Supporting Information Fig.S6A).

P300 occupancy highly correlates with active enhancers [44]. As a next step, we identified the P300 occupied genomic regions in the close proximity of the 398 PRMT1-sensitive RA regulated genes (see Fig.3A) to identify putative common master regulators of these genes. The motif analysis of these genomic regions revealed the enrichment of Oct3/4, Sox2 and Nanog beside the RAR:RXR bound NR half site (Fig.3I). Interestingly, comparison of promoter regions of PRMT1-insensitive (eg. Cyp26a1, Dleu7, Rbp1, Stra8, Dhrs3) and PRMT1-sensitive (eg. Hoxa1, Hoxb1, Spsb1, Pmp22, Stra6 and Foxd3, Otx2, Zfp428, Fgf5) genes showed remarkable differenes in the overall enrichment of Oct3/4, Sox2 and Nanog (Fig.3J). Moreover, P300 redistribution could also only be detected on promoter region of PRMT1-sensitive genes (Fig.3J, Supporting Information Fig.S6B and S6C), suggesting that P300 and PRMT1 are likely to co-regulate such transcriptional “hotspots”.

To get further mechanistic evidence that these regions are targeted by PRMT1, we determined the H4R3me2a signal in the proximity of PRMT1-sensitive and insensitive genes. As shown in Fig.3K and Supporting Information Fig.S6D, Hoxa1, Spsb1, Otx2 and Zfp428 enhancers showed clear PRMT1-dependent enrichment of H4R3me2a at these regions, while P300 recruitment was not altered (Fig.3L and Supporting Information Fig.S6E). RA-dependent changes showed no clear tendency between the compared regions (Supporting Information Fig.S6F, S6G). In accordance with the P300 ChIP-seq data ChIP-qPCR validation confirmed that RA treatment selectively increased the recruitment of P300 to the promoter of Hoxa1 but not to Cyp26a1 or Dhrs3 (Fig.3M and Supporting Information Fig.S6H, S6I). Spsb1 already showed increased P300 binding which was not further enhanced (see also Fig. 3J) As expected, Otx2 and Zfp428 showed decreased P300 binding upon RA treatment (Supporting Information Fig. S6H and S6I). Interestingly, we detected a constant Oct3/4 binding on the Hoxa1 enhancer even after 24h of RA treatment (Fig. 3M), while Oct3/4 occupancy has significantly decreased on the enhancer of repressed Otx2 (Fig. 3N). These data collectively suggest that RA reguleted enhancers can be grouped into PRMT1 sensitive and insensitive ones with distinct transcription factor complexes. The PRMT1 sensitive ones are characterized by PRMT1-dependent H4R3me2a, OSKN and P300 binding.

**PRMT8 is a retinoic acid inducible co-activator of retinoid signaling**

As it was shown in Figure 1C, retinoic acid treatment resulted in changes in asymmetric arginine methylation. Comparison of the expressional profile of PRMTs upon short-term RA-induction of day 4 EBs revealed the early upregulation of PRMT8 (Fig.4A and 4B). To prove that PRMT8 is regulated in a RA-dependent manner, ESCs were treated with RAR and RXR specific ligands. PRMT8 expression could be induced by RAR specific ligand AM580, but as expected RXR

specific LG268 had no effect (Supporting Information Fig.S7A). Moreover, RA-dependent induction of PRMT8 showed a similar time- and dose dependence as Hoxb1 and Cyp26a1, well-known direct targets of the retinoid signaling pathway (Fig.4B, Supporting Information Fig.S7B and S7C) [45]. A recently published RAR ChIP-seq in F9 cells [46] allowed us to identify a putative enhancer in the promoter region of PRMT8. This region (-1400 to -1450 relative to TSS) contains a direct repeat with no spacer (AGGTCAAGGTCA, DR0), that can bind RAR:RXR (Supporting Information Fig. S7D). Transfecting an enhancer trap vector that contains this ~300bp genomic region of the PRMT8 promoter, we could validate functionally the element in response to RA treatment in ESCs (Fig.4C). These results confirm PRMT8 as a direct RA-regulated gene. Importantly, using the same construct, we could not detect RA-dependent induction of PRMT8 in HEK293T cells (Fig.4C). This suggests a more complex scenario, where the presence of additional cell-type specific factors are required for proper enhancer activity.

PRMT1 and PRMT8 exhibit high sequence similarities [25], thus we were interested whether loss of PRMT8 may also affect retinoid response. Unexpectedly, loss of PRMT8 had an inhibitory effect on the retinoid response. In a dose-curve comparison of Hoxb1 and Cyp26a1 induction loss of PRMT8 resulted in a significant increase in the half maximal effective concentration (EC50) value of RA (Hoxb1: 4.8nM to 860nM, Cyp26a1: 148nM to 808nM) (Fig.4D). To validate the co-regulatory function of PRMT8 in RAR:RXR signaling, enhancer trap vectors of Hoxb1 or Cyp26a1 RARE were used in a luciferase reporter assay (see Supporting Information Fig. S5D). As shown in Figure 4E, ESCs transfected with the reporter alone showed RA-dependent induction, which was further stimulated by co-transfection of PRMT8. In contrast, loss of PRMT8 resulted in a decreased signal intensity (Fig.4F). Moreover, the decrease observed in PRMT8-depleted cells could be restored by the overexpression of PRMT8 (Supporting Information Fig.S7E). In contrast to PRMT1, loss of PRMT8 also resulted in a decrease in the

signal when an artificial canonical DR2 containing reporter was used (Fig.4G), suggesting that PRMT8 is a general co-activator of RA signaling. To dissect the role of PRMT1 and PRMT8, we used PRMT8 depleted cells on PRMT1-/- background (double knockdown). The inhibitory effect in the absence of PRMT8 was found to be independent of the presence of PRMT1 (Fig.4H).

**PRMT1 and PRMT8 regulate subtype specification of differentiating neural cells**

Next, we studied if loss of either or both PRMT1 and/or PRMT8 has consequences on retinoic acid induced neuronal differentiation and/or gene expression. The stability of the knockdowns has been confirmed in differentiated neurons (Fig.5A, Supporting Information Fig.S8A). Importantly, loss of either PRMT1 or PRMT8 resulted in hypomethylation of neurons as detected by anti-ASYM24 antibody (Fig.5A).

At day 12 of differentiation the knockdown derived neural cells showed similar morphology and high expression of typical neural markers, such as Lhx1, Pax6 or Tuj1 to wild-type cells (Fig.5B, Supporting Information Fig.S8B). PRMT1 knockout cells could also differentiate to TUJ1+ neurons (Supporting Information Fig.S8C), further demonstrating that PRMT1 is not an essential factor in early neural differentiation. In contrast, genome-wide analysis of day 16 samples revealed dysregulation of several genes in PRMT1 or PRMT8-depleted cells (Fig.5C). Loss of either PRMT1 or PRMT8 resulted in mainly the downregulation of genes. Interestingly, grouping of the differentially expressed genes identified that a large fraction of the genes (473 out of 947) showed similar dysregulation in both knockdown cell types (Fig.5D). We validated Phox2b (Paired-Like Homeobox 2b), an important transcription factor of neural specification [47] and Gfra2 (GDNF Family Receptor Alpha), a regulator of neurite outgrowth [48] by RT-qPCR (Fig.5E). Gene expression data suggested that PRMT1 and PRMT8 might act together in the

regulation of these genes. Indeed, as shown in Figure 5F, co-immunoprecipitation studies confirmed that the two proteins are likely present in one complex.

To further evaluate the characteristics of early progenitors and differentiated neurons, we compared the ratio of dividing vs. non-dividing cells. In the progenitor phase mitotic index of PRMT1-depleted cells were significantly higher (Fig.5G). Cell cycle analysis of differentiated cells at day 16 also suggested that PRMT1-depleted cells show significantly higher number of non-terminally differentiated, dividing cells (Fig.5H).

Importantly, expression level of ES markers and mesoderm, endoderm or early ectoderm lineage markers were similarly low in neurons differentiated from hypomethylated cells (Supporting Information Fig.S8D-F), further confirming that loss of PRMT1 and PRMT8 do not inhibit the neural differentiation per se. Ingenuity pathway analysis of the 473 genes (Fig.5D) implicated PRMT1 and PRMT8 in neuronal synaptic formation, glutamate receptor signaling and axonal guidence (Supporting Information Fig.S8G). Next, we studied functional properties of PRMT1 or 8-depleted neurons by calcium imaging. This method allowed us to compare >200 cells per condition. Importantly, the frequency of calcium peaks and the frequency of action potentials recorded in the same neuron showed a significant correlation (Supporting Information Fig.S9A), in accordance with earlier observations [28, 49, 50]. Approximetly 50% of the cells showed neural activity in the control and PRMT8 knockdown cells, while in the PRMT1-depleted cell culture the rate of active cells was almost 100% (Fig.5I). As a remarkable difference, we found that the frequency of fast calcium signals per active cells was dramatically dropped in PRMT8-knockdowns, suggesting an important role of PRMT8 in the establishement of neuronal excitability (Fig.5J). Another interesting observation was the frequent occurance of synchronous activity among the cells of the PRMT1 knockdown cultures (see synchronous events labelled with asterisks in Fig.5K).

**PRMT8 regulates distinct set of genes and loss of PRMT8 is a marker of glioblastoma multiforme**

The gene expressional analysis also revealed that several genes, such as Cxcr4, Dhfr or Efemp1 previously linked to glial differentiation and gliomagenesis [51-53] were expressed differentially only in PRMT8 knockdown cells (Fig.6A and 6B). Using PRMT1-PRMT8 double knockdown cells we found that these genes are PRMT8-dependent (Fig.6C-E).

We used a large number of human primary glioma samples to confirm that PRMT8-dependent Cxcr4 and Efemp1 indeed show dysregulation in glioblastoma multiforme (GBM) (Fig.6F). Prompted by this finding and a result of a recent study that linked SNP variation in PRMT8 promoter to familial gliomagenesis [54] we also determined expression of PRMT8 in these samples. Very strikingly, PRMT8 itself showed a substantially lower expression level in GBM samples, while PRMT1 did not show a difference between the groups (Fig.6F). These data indicate that loss of PRMT8 and genes regulated by it are putative markers in GBM and might participate in its development.

## 4. Discussion

We combined genetic approaches with genome-wide gene expression technologies to unravel the contribution of PRMT1 and PRMT8 to *in vitro* neuronal differentiation. We propose the following model (Fig. 6G). There are two distinct phases during the course of neural differentiation: in early stages only PRMT1 is expressed. PRMT1 acts as a selective repressor of a large set of retinoic acid induced genes (Hoxa1, Hoxb1, Pmp22 and Spsb1). The promoter regions of these PRMT1-sensitive genes are regulatory “hotspots” as they are occupied by Oct3/4, Sox2, Klf4 or Nanog (OSKN) and show P300 recruitment upon RA-treatment. Genes,

such as Otx2 and Zfp428, that are active in ESCs and occupied by OSKN and P300 are also influenced by PRMT1. This way PRMT1 arms the cells with a negative-feedback mechanism to limit RA's effect on a subset of target genes.

Subsequently, the RA signal directly induces the expression of PRMT8. In this late stage, PRMT8 collaborate with PRMT1, but PRMT8 might also exist as a homodimer [25]. PRMT8 in such complex acts as a co-activator that potentiates retinoid response. In this way PRMT1 and its closest paralogue PRMT8, integrate the morphogenic RA signal in a temporal manner acting as a rheostat. Loss of PRMT1 or PRMT8 results in mostly similar changes in neural specification, but PRMT1and PRMT8 have independent regulatory potential as well.

PRMT1 has been previously identified as a ubiquitously expressed secondary co-activator for nuclear receptors. It has been also shown to bind the activation domain (AD2) of primary co-activators and enhance transcription [10]. In contrast to this, our results now show a repressive function of PRMT1, confirming in principle the findings of previous studies providing evidence for co-repressor roles for PRMT1 in different cellular context [55, 56]. These opposing roles in gene expression regulation are not unique to PRMT1, similar phenomenon has been reported in case of other co-activators as well [57].

Gene and enhancer selectivity is also a novel and striking feature of PRMT1, however the exact mechanism remained unclear. Strikingly, PRMT1-sensitive sites show characteristics of cell-type specific regulatory "hotspots" [58]: key transcription factors, such as Oct3/4, Sox2, Klf4 and Nanog are enriched and mark these genomic regions. Importantly, the co-activator P300 is also selectively recruited to these sites upon RA-treatment, providing further evidence to the existence of distinct epigenetic states between PRMT1-sensitive and insensitive sites. We found no indication that loss of PRMT1 would affect P300 recruitment to these "hotspots", but we could detect a remarkable decrease in the level of H4R3me2a mark at these sites in PRMT1-depleted

cells, suggesting the presence of PRMT1 at these sites. PRMT1-insensitive regions did not show PRMT1-dependent H4R3me2a enrichment, however few exceptions could be noticed (eg. Rarβ). Due to the lack of reliable ChIP-grade anti-PRMT1 antibody, we could not get reproducible data so far which would provide direct evidence for the presence of PRMT1 at these sites though. A potential mechanism for the enhancer selective effect of PRMT1 is that P300 or a member of this protein complex is arginine methylated and this affects its co-activator function. This possibility would also explain why only P300 recruiting genomic regions are PRMT1-sensitive. Such arginine methylation dependent regulation of CBP has been demonstrated by others [37, 38] and we also could detect the presence of arginine methylated proteins in the P300 complex. Further studies will be required to evaluate this possibility in neuronal differentiation.

The result of loss of PRMT1 function in differentiation neurons is altered gene expression. Gene expression data obtained can be used in further studies to mechanistically describe the PRMT-dependent transcriptional network in neurogenesis. Importantly, the detected gene expressional differences could be linked to various functional defects. First, we found that loss of PRMT1 resulted in a delay in the cell cycle exit and elevated number of mitotically active cells. These finding are in line with a study which has identified the dominantly PRMT1-mediated H4R3me2a as a marker of post-mitotic neurons [59].

A recent study identified methylation of brain sodium channel Nav1.2 in response to seizures [60]. Our preliminary comparison of electrophysiological properties of the knockdown cells led us to the conclusion that PRMT1 and PRMT8 likely responsible for the proper function of ion channels. Further *in vitro* and animal studies will be required to identify more precisely the functional consequences of loss of these PRMTs.

Dysregulation of RA-signaling has also been implicated in disease emergence and progression [61]. It is an intriguing question whether PRMT1 and PRMT8 are involved in pathological conditions of the brain as well. Our pathway analysis indicates a role of PRMT1 and PRMT8 in MAPT (microtubule-associated protein tau), APP (amyloid beta A4 protein), PSEN1 (presenilin 1) and BDNF (brain-derived neurotrophic factor) related pathways. Moreover, several genes showing dysregulated expression in knockdowns have been also identified in a recent study as potential markers of human AD [62] (Supporting Information Fig.S9B and S9C). As PRMT1 or PRMT8 expression has not been investigated in such disease conditions it is still very tentative to suggest PRMT1 and PRMT8 in the progression of AD. However the observed gene expression pattern propound further *in vivo* correlative as well as mechanistic studies.

A previous comparison of mammalian PRMTs revealed that PRMT1 and PRMT8 share the highest degree of identity within this enzyme family [25]. Not only the amino acid sequence of the two proteins, but also the intron-exon boundaries are well conserved, suggesting that PRMT8 evolved by the duplication of PRMT1. Importantly, a recent study demonstrated that despite the similarities, PRMT1 and PRMT8 have non-redundant functions in the neural development of Zebrafish [63], suggesting that PRMT8 has acquired novel functions since its duplication. Our genome-wide screen and double knockdown experiments also provide evidence of a PRMT1-independent program of PRMT8.

Dysregulation of RA-signaling has been also implicated in progression of different subtypes of cancers [64]. In a recent study, up-regulation of PRMT1 has been reported in glioma tissues and glioma cell lines [65]. In order to revisit this issue we used a large patient cohort and found that the RNA levels of PRMT8 are almost completely down-regulated in glioma tissues. A trivial explanation may be that PRMT8, a highly specific neural marker, is not expressed in astrocyte-derived tumors [66]. Alternatively, loss of PRMT8 positively affects astrocyte differentiation,

resulting in a shift in cell fate commitment. Further *in vivo* and *in vitro* studies are required to provide evidence to this. Our results show that loss of PRMT8 results in a decrease in the level of Gfra2 and increase in the level of Cxcr4, Dhfr and Efemp1 in a single and double knockdown cells as well. These are established markers of astrocyte-derived glioma [52, 67, 68]. Furthermore, a recent genome-wide linkage study of glioma families linked a PRMT8 related SNP to gliomagenesis [54]. Downstream effect of this SNP has not been linked to the expression of PRMT8 yet. Although further work is required, these results already provide strong support to the notion that PRMT8 might be a genetic risk factor in gliomagenesis and also a putative therapeautic target. Regardless of the mechanism, our results implicate PRMT8 as a biomarker of glioma tissues.

## 5. Conclusions

In summary, the results of this study suggest a novel and so far unprecedented mechanism of how two evolutionary linked proteins with similar enzymatic activity can have distinct effects on cellular differentiation through the integration of retinoid signaling acting as parts of a rheostat. These results provide a new conceptual framework for the interpretation of retinoid signaling in neuronal differentiation and potentially in other tissues as well. These proteins, PRMT1 and PRMT8, can also be targeted pharmacologically to modulate neuronal differentiation *in vitro* or *in vivo* and might also be a relevant target in a major unresolved clinical issues such as gliomas and Alzheimer's disease.

## 6. Acknowledgement

The authors would like to acknowledge Dr. Istvan Szatmari and members of the Nagy laboratory for discussions and comments on the manuscript. We thank Ibolya Furtos, Beata Szalka, Marta

Beladi, Imrene Molnar and Zoltanne Karolyi for technical assistance. We thank Dr. Andras Dinnyes and Julianna Kobolak (Agricultural Biotechnology Center, Godollo, Hungary) for help with ES work. L.N is supported by a grant from the Hungarian Scientific Research Fund (OTKA K100196), TÁMOP422_2012_0023 VÉD-ELEM implemented through the New Hungary Development Plan co-financed by the European Social Fund and the European Regional Development Fund and Hungarian Brain Research Program – Grant No. KTIA_13_NAP-A-I/9. Z.S is a recipient of TÁMOP-422/B10/1_2010_0024 grant and supported by TÁMOP 4.2.4. A/2-11-1-2012-0001/A2-JÁDJ-13. BLB was supported by a grant from the Hungarian Scientific Research Fund (OTKA F68254) and Bolyai, Zoltan Magyary and the Szodoray Fellowships. I.J. was supported by a grant from TÁMOP- 4.2.2.A-11/1KONV-2012-0023.

Library preparation and bioinformatic analysis was performed at the Center of Clinical Genomics and Personalized Medicine of the University of Debrecen. RNA-sequencing was performed at the Centre National de Genotypage (CNG) Paris, directed by Jean-Francois Deleuze and supported by the European Sequencing and Genotyping Infrastructure (funded by the European Comission, FP7/2007-2013) under grant agreement no. 26205 (ESGI), as part of the ADIPOMACS transnational access programme.

## 7. Disclosure of Potential Conflicts of Interest

The authors indicate no potential conflicts of interest.

## 8. Figure legends:

**Figure 1.** Asymmetric arginine methylation is changing in distinct stages of retinoic acid induced neural differentiation

(A) Flow diagram of the multistage differentiation procedure that involves: (I) undifferentiated stem cell culture, (II) embryoid body formation, (III) all-trans retinoic acid (RA) treatment and (IV) neuronal culture on Poly-L-ornithin/laminin-coated plates. Indicated stages are shown with bright field microscopy.

(B) Typical single-cell voltage clamp and current clamp measurements of terminally differentiated (day 16) neurons. Upper panel: Voltage-gated inactivating and non-inactivating inward currents (from -30mV) are marked on the figure. Lower panel: ESC-derived neurons were used in depolarising current injection steps. AP-trains with over-shoot are shown.

(C) Immunoblot analysis of different stages of neural differentiation. Samples were collected at day 0, 4, 8, 12 and 16 of neural differentiation. Anti-ASYM24 antibody recognizes proteins that contain arginines that are asymmetrically dimethylated. Anti-SYM11 antibody recognizes proteins that contain arginines that are symmetrically dimethylated. GAPDH serves as a loading control.

(D) Genome browser view of the merge of mESC RNA-seq, and RNA Pol and H3K27ac ChIP-seq activity on the indicated loci.

(E) Expression profile of PRMTs as detected by RT-qPCR. RNA samples were collected at day 0 (I), day 4 (II), day 8 (III) and day 12 (IV). Gene expression data are expressed as a ratio of the indicated genes' transcript relative to Gapdh.

(F) Total intranuclear levels of Histone 4 aRginine 3 asymmetric dimethylation as compared by indirect immunofluorescence, on a cell-by-cell basis, by laser scanning cytometry. The columns show the means of the fluorescence intensity distribution histograms obtained for G1 cells in four independent experiments ($p \leq 0.001$). The bars on the columns are SDs.

(G) Immunoblot analysis of different stages of neural differentiation. Samples were collected at day 0, day 4, day 8 (+/- RA treatment) and day 12 (+/- RA treatment). GAPDH serves as a loading control.

(H) Localization of H4R3me2a, PRMT1 and PRMT8 (each in red) in stem cell derived neuronal cells as detected by immunocytochemistry. Neurons were co-stained by anti-TUJ1 antibody (green). Arrows indicate the cytoplasmic localization of PRMT1.

ns - non significant, *P ≤0.05, **P ≤0.01 *** P ≤0.001

Abbreviations: LIF, leukemia inhibitory factor; βME, beta-mercaptoethanol; FBS, fetal bovine serum.

**Figure 2.** PRMT1 is responsible for arginine methylation in ESCs and affects transcription

(A) Genome browser view of RNA-seq data comparing the PRMT1 coding locus in the indicated ESCs. Biological duplicates are shown.

(B) Immunoblots of protein samples from the indicated D3 ESCs lines; probed for expression of PRMT1, ASYM24 and OCT3/4. ACTIN was used as a loading control.

(C) Western blot analysis of subcellular fractionations. Cytoplasmic (CYTO) and nuclear fractions (NUC) of undifferentiated shSCR and shPRMT1 ESCs were isolated and probed for PRMT1 and ASYM24. GAPDH is a loading control for cytoplasm.

(D) Total intranuclear levels of H4R3 asymmetric dimethylation as compared by indirect immunofluorescence between undifferentiated shSCR and shPRMT1 ESCs.

(E) Characterization of unmodified D3, shSCR, shPRMT1 and shPRMT8 ESCs. Expression of ES marker SSEA-1 and OCT3/4 were determined by immunocytochemistry. Alkaline

Phosphatase (AP) staining show undifferentiated colonies. Chromosome counting was performed as described in the Supporting Information.

(F) Heatmap display of gene expression data of D3, E14 and PRMT1-/- ESCs, normalized to D3 and shSCR vs shPRMT1 ESCs, normalized to shSCR. Total RNA was isolated from undifferentiated ESCs and RNA-seq experiment was carried out to determine those genes that were significantly (FDR $\leq$0.1 and Log2FC $\geq$1.2) up-regulated (n=39, red), or down-regulated (n=126, blue) in both PRMT1-/- and shPRMT1 ESCs vs. their control. See also Supporting Table 1.

(G) Asym24 immunoblot of P300 interacting complex. Nuclear extract of control and PRMT1-depleted cells were used to co-immunprecipitate proteins with anti-P300 or IgG isotype control.

(H) *De novo* identification of motifs under peaks from P300 ChIP-seq data using Homer. Top 1000 binding sites in each samples and the matrix files of the best motifs (highest score) were used for forced motif search in D3 shSCR and E14 shSCR P300 ChIP-seq samples. % refers to the ratio of peaks having the given motif.

(I) Histogram of PRMT1-dependent P300-binding. P300 ChIP-seq was carried out in shSCR and shPRMT1 D3 and E14 ESCs. Regions showing significantly different ($p<0.05$) P300 occupany between shSCR and shPRMT1 in both D3 and E14 were identified by differential binding analysis, resulting 40 up- (red) and 47 down-regulated (black) P300 occupied genomic regions in shPRMT1 (dashed line) vs shSCR (continual line).

(J) Hematoxylin and eosin staining of teratoma derived from PRMT1-/- ESCs. Cells were injected into lower leg of SCID mice at a concentration of $5x10^6$ cells ml-1.After 4~6 weeks the teratoma were surgically dissected, fixed, embedded in paraffin and sectioned.

(K) Ingenuity pathway analysis of genes differentially expressed at day 4. Microarray experiment was carried out using RNA samples obtained from shSCR and shPRMT1 ESCs differentiated for 4 days. Top biological functions predicted by the software and p-values are shown.

ns - non significant, *P ≤0.05, **P ≤0.01 *** P ≤0.001

Abbreviations: AP, alkaline phosphatase.

**Figure 3.** PRMT1 acts as selective regulator of retinoid regulated genes

(A) Proportional Venn-diagram that represents the overlap between gene expression changes in retinoid induced differentiation of control (shSCR) and PRMT1-depleted cells as determined by microarray. Embryoid bodies at day 4 were treated with DMSO or 5μM retinoic acid (RA) for 12h.

(B) Gene expression changes from control and PRMT1-depleted cells upon RA-treatment. Cells were spontaneously differentiated for four days and then treated with RA or vehicle for 12h. Fold inductions were calculated from per chip normalized microarray data (vehicle vs. RA treated, n=3 per condition) for each gene. Calculated values of PRMT-depleted cells then were normalized by values of the control. Red line shows when the induction is equal in both cell types (eg. Cyp26a1, Dhrs3).

(C) PRMT1-dependent repression of retinoic acid-induced enhancers. pcDNA.3.1-PRMT1 (PRMT1) or empty pcDNA3.1 (empty) plasmids were co-transfected with NHf290-Hoxb1-Luciferase plasmid[41] or Pmp22 and Spsb1 enhancers cloned into Luciferase encoding vector (see Supporting Information Fig.S5C). Luciferase signal intensity was determined and normalized to βgal signal.

(D) RA-dependent activation of Hoxb1 promoter and Spsb1 enhancer. Indicated plasmids were co-transfected with NHf290-Hoxb1-Luciferase or Spsb1-Luciferase plasmid and cells were treated with RA.

(E) NHf-Hoxb1-Luciferase plasmid was transfected into shSCR or shPRMT1 cells. Cells were treated with RA for 24h using the indicated ligand concentration and normalized luciferase values determined.

(F) DR2 retinoic acid response element containing luciferase plasmid was co-transfected with pcDNA3.1-empty or pcDNA3.1-PRMT1 expression vector. Cells were treated with RA for 24h using the indicated concentrations.

Normalized luciferase activity was determined and the mean of triplicate determinations +/- SD is shown.

(G) Area-proportional Venn-diagram of RA induced P300 redistribution. Cistromes of P300 were determined in control (vehicle) and RA-treated (1μM, 24h) D3 shSCR ES cells by ChIP-seq.

(H) Histogram of the genome-wide occupancy of common P300 peaks (n=1103) in vehicle and RA-treated (1μM, 24h) cells, centralized to common P300 occupied regions.

(I) *De novo* identification of motifs under P300 peaks from ChIP-seq data using Homer. P300 occupied genomic regions were identified in promoter regions of the 398 PRMT1-sensitive RA-regulated genes (see Fig.3A). % of targets refers to the ratio of peaks having the given motif.

(J) Genome browser view of the indicated ChIP-seq data on PRMT1-sensitive and PRMT1-insensitive loci. H3K27ac, RXR and P300 ChIP-seq data were obtained from untreated ESCs and cells treated with 1μM RA for 24h.

(K) H4R3me2a ChIP-qPCR signals on the indicated individual enhancers (see Fig.3J) as detected in untreated shSCR, shPRMT1 and shPRMT8 ESCs.

(L) P300 ChIP-qPCR signals on the indicated individual enhancers as detected in untreated shSCR, shPRMT1 and shPRMT8 ESCs.

(M) RAR, RXR, P300 and Oct3/4 ChIP-qPCR signals on the Hoxa1 enhancer (see Fig.3J) in undifferentiated and RA-treated ESCs.

(N) P300 and Oct3/4 ChIP-qPCR signals on the Otx2 enhancer (see Fig.3J) in undifferentiated and RA-treated ESCs.

ns - non significant, *P ≤0.05, **P ≤0.01 *** P ≤0.001

Abbreviations: DR, direct repeat; Luc, luciferase; wt, wild-type; veh, vehicle.

**Figure 4.** PRMT8 is a Retinoic Acid Receptor regulated gene and acts as a co-activator of retinoid signaling

(A) Heatmap analysis of gene expression microarray data of PRMT family members. Values are normalized to undifferentiated ESCs (day 0).

(B) Ligand response of PRMT8 upon RA treatment at various time points. Undifferentiated ESCs were treated for the indicated times with 1μM RA.Values are expressed as mean of technical triplicates ± SD of the mean.

(C) TK-Luc-PRMT8 was constructed by cloning ~300bp promoter region of PRMT8, containing the DR0 element, into a TK-Luc-empty plasmid. ESCs or HEK293T cells were transiently transfected and treated with 0.1μM RA for 24h. Above the identified DR0 element and surrounding sequence is shown.

(D) Dose response curves of Hoxb1 and Cyp26a1 as measured by RT-qPCR. shSCR and shPRMT8 ESCs were treated with the indicated concentrations of RA for 24h. EC50 values are shown.

(E) TK-Luc Hoxb1 or TK-Luc Cyp26a1 enhancer traps were constructed by cloning ~300bp regions of Hoxb1 and Cyp26a1, respectively (see Supporting Information Fig.S5D). ESCs were transfected along with pCMV-Tag2-empty or pCMV-Tag2-PRMT8 expression plasmid. Cells were treated with RA for 24h using the indicated ligand concentrations.

(F) Hoxb1 (DR2) or Cyp26a1 (DR5) enhancer trap was transfected into shSCR or shPRMT8 ESCs. Cells were treated with RA for 24h using the indicated ligand concentrations.

(G) 2xDR2 retinoic acid response element containing luciferase plasmid was transfected into shSCR or shPRMT8 ESCs. Cells were treated with RA for 24h using the indicated ligand concentrations.

(H) 2xDR2 retinoic acid response element containing luciferase plasmid was transfected into PRMT1 knockout (P1-/-) or shPRMT8 PRMT1 double "knockout" (P1-/- shP8) ESCs. Cells were treated with RA for 24h using the indicated ligand concentrations. Normalized luciferase values were determined and the mean of three determinations +/- SD are shown.

ns - non significant, *P ≤0.05, **P ≤0.01 *** P ≤0.001

Abbreviations: EC50, half maximal effective concentration; DR, direct repeat; P1-/- /shP8, PRMT1 knockout / shPRMT8.

**Figure 5.** PRMT1 and PRMT8 affect neuronal differentiation

(A) Immunoblot analysis of day 16 differentiated neurons derived from the indicated cell types probed for the indicated proteins.

(B) TUJ1-staining of day 12 neurons. DAPI co-staining was used to visualize cell nuclei.

(C) Heatmap display of microarray gene expression data obtained from D3, shSCR, shPRMT1 and shPRMT8-derived neurons at day 16, normalized to D3 neurons. Hierarchical cluster

analysis is shown. Blue color indicates downregulated, red shows upregulated genes compared to D3-derived neurons.

(D) Area-proportional Venn-diagram compares PRMT1-dependent and PRMT8-dependent gene expression changes in differentiated neurons. Cells differentiated for 16 days were used for microarray experiments. Significantly changing genes (FC≥1.5, $p<0.05$) were determined by comparing shSCR vs. shPRMT1 or shSCR vs. shPRMT8-derived neurons.

(E) RT-qPCR validation of expression level of Phox2b and Gfra2 in the indicated cells.

(F) Co-immunoprecipitation of PRMT1 by full-length FLAG-PRMT8. HEK293T cells were transfected with the indicated constructs. Anti-MYC antibody was used for immunoblot analysis.

(G) Mitotic index of day 8 embryoid bodies were evaluated and compared by counting mitotic figures on H&E-stained slides. A representative mitotic figure and a rosettoid structure are shown. Average number of mitotic figures per 20 consecutive high-power fields (HPF, 40x magnification) is shown.

(H) Cell cycle analysis of the differentiated shSCR, shPRMT1 and shPRMT8 knockdown cells. Nuclei of agarose embedded and permeabilized cells were stained with propidium iodide and measured by laser scanning cytometry. In the left panel, the bar charts show the percentage of cells in the different cell cycle phases. Error bars: SD calculated from n≥3 independent experiments. The dot-plots and DNA histograms (right panel) show one representative measurement for each cell line. In the case of shSCR and shPRMT1 neurons, the difference between the ratio of non-dividing and dividing cells ((G1+G0)/(S+G2+M)) was statistically significant (p=0,029; Mann Whitney rank sum test).

(I) Ratio of cells with recorded fast calcium signal. Recordings and analysis has been carried out in the indicated ESC-derived neural cultures. A representative experiment is shown (>200 measured neurons/condition).

(J) Counts of calcium signals per minute normalized to the number of cells with positive calcium signal. A representative experiment is shown (>200 measured neurons/condition).

(K) Synchronous activity among the cells of the PRMT1 knockdown cultures. Synchronous events labelled with asterisks. Calcium imaging records of 6 randomly chosen ROIs / condition are shown.

ns - non significant, *P ≤0.05, **P ≤0.01 *** P ≤0.001

Abbreviations: WB, Western Blot; IP, Immunoprecipitation; HPF, high-power fields.

**Figure 6.** Loss of PRMT8 results in a gene expression profile that resemble neurological disorder

(A) Heatmap visualization of microarray data of the indicated glioma releated markers in ES-derived neurons. Cells differentiated for 16 days were used for microarray experiments and data was normalized to wt D3-derived neurons.

(B) Gene expression level of Cxcr4 and Dhfr as measured by RT-qPCR in day 16 ESC-derived neurons.

(C) Gene expression level of PRMT8 in PRMT1 -/- shSCR vs. PRMT1 -/- shPRMT8 ESC-derived neurons as measured by RT-qPCR at day 12 of differentiation.

(D) Immunoblot analysis of TUJ1 in different stages of PRMT1 -/- shSCR vs. PRMT1 -/- shPRMT8 neural differentiation. Samples were collected at day 8, 12 and 16. GAPDH serves as a loading control.

(E) Gene expression level of indicated genes in PRMT1 -/- shSCRvs PRMT1 -/- shPRMT8 ESC-derived neurons as measured by RT-qPCR at day 14 of differentiation.

(F) Gene expression level of Cxcr4, Efemp1, PRMT1 and PRMT8 as measured by RT-qPCR. Human normal (n=54) and glioblastoma multiforme (GBM) (n=83) samples were compared. Each dot represents an individual sample.

(G) Proposed model of PRMT1 and 8's action on early and late stage of neuronal differentiation. PRMT1 is expressed in early stage and acts as a selective repressor of retinoic acid induced gene expression. PRMT1-sensitive (eg. Hoxb1) regions are occupied by Oct3/4, Sox2, Klf4 or Nanog, while PRMT1-insensitive sites (eg. Cyp26a1) are not enriched for these transcription factors. P300 is also selectively recruited to the PRMT1-sensitive sites only. H4R3me2a marks can be detected in a PRMT1-dependent manner on the close proximity of all these PRMT1-sensitive enhancers. PRMT1-sensitive, RA-repressed genes (eg. Otx2) also show P300 and OSKN occupancy in untreated ESCs. In the late stage, RA-induced PRMT8 are present in a complex with PRMT1 but PRMT8 might also exist as a homodimer [25]. PRMT8 in such complexes acts as a co-activator that potentiates retinoid response. Hox-genes, Mapt and Phox2b are regulated by both PRMT1 and PRMT8. Pathway analysis predicts REST, MAPT, APP, PSEN1 as upstream regulators responsible for dysregulated gene expression. PRMT8 has a PRMT1-independent regulatory potential as well, affecting gliomagenesis-related genes, such as Cxcr4, Dhfr or Efemp1.

## 9. References


1. Thaller C, Eichele G. Identification and spatial distribution of retinoids in the developing chick limb bud. **Nature**. 1987;327:625-628.
2. Shimozono S, Iimura T, Kitaguchi T et al. Visualization of an endogenous retinoic acid gradient across embryonic development. **Nature**. 2013.
3. Chambon P. The nuclear receptor superfamily: a personal retrospect on the first two decades. **Mol Endocrinol**. 2005;19:1418-1428.
4. Koide T, Downes M, Chandraratna RA et al. Active repression of RAR signaling is required for head formation. **Genes Dev**. 2001;15:2111-2121.
5. Glass CK, Rosenfeld MG. The coregulator exchange in transcriptional functions of nuclear receptors. **Genes Dev**. 2000;14:121-141.
6. Rochette-Egly C. Dynamic combinatorial networks in nuclear receptor-mediated transcription. **J Biol Chem**. 2005;280:32565-32568.
7. Lonard DM, O'Malley B W. Nuclear receptor coregulators: judges, juries, and executioners of cellular regulation. **Mol Cell**. 2007;27:691-700.
8. Xie Y, Ke S, Ouyang N et al. Epigenetic regulation of transcriptional activity of pregnane X receptor by protein arginine methyltransferase 1. **J Biol Chem**. 2009;284:9199-9205.
9. Rizzo G, Renga B, Antonelli E et al. The methyl transferase PRMT1 functions as co-activator of farnesoid X receptor (FXR)/9-cis retinoid X receptor and regulates transcription of FXR responsive genes. **Mol Pharmacol**. 2005;68:551-558.
10. Koh SS, Chen D, Lee YH et al. Synergistic enhancement of nuclear receptor function by p160 coactivators and two coactivators with protein methyltransferase activities. **J Biol Chem**. 2001;276:1089-1098.
11. Balint BL, Szanto A, Madi A et al. Arginine methylation provides epigenetic transcription memory for retinoid-induced differentiation in myeloid cells. **Mol Cell Biol**. 2005;25:5648-5663.
12. Gayatri S, Bedford MT. Readers of histone methylarginine marks. **Biochim Biophys Acta**. 2014.
13. Lee YH, Ma H, Tan TZ et al. Protein arginine methyltransferase 6 regulates embryonic stem cell identity. **Stem Cells Dev**. 2012;21:2613-2622.
14. Wu Q, Bruce AW, Jedrusik A et al. CARM1 is required in embryonic stem cells to maintain pluripotency and resist differentiation. **Stem Cells**. 2009;27:2637-2645.
15. Nakajima T, Matsuoka Y, Kakimoto Y. Isolation and identification of N-G-monomethyl, N-G, N-G-dimethyl- and N-G,N' G-dimethylarginine from the hydrolysate of proteins of bovine brain. **Biochim Biophys Acta**. 1971;230:212-222.
16. Miyata S, Mori Y, Tohyama M. PRMT1 and Btg2 regulates neurite outgrowth of Neuro2a cells. **Neurosci Lett**. 2008;445:162-165.
17. Pawlak MR, Scherer CA, Chen J et al. Arginine N-methyltransferase 1 is required for early postimplantation mouse development, but cells deficient in the enzyme are viable. **Mol Cell Biol**. 2000;20:4859-4869.
18. Cimato TR, Tang J, Xu Y et al. Nerve growth factor-mediated increases in protein methylation occur predominantly at type I arginine methylation sites and involve protein arginine methyltransferase 1. **J Neurosci Res**. 2002;67:435-442.
19. Tsai YJ, Pan H, Hung CM et al. The predominant protein arginine methyltransferase PRMT1 is critical for zebrafish convergence and extension during gastrulation. **FEBS J**. 2011;278:905-917.

20. Bedford MT, Clarke SG. Protein arginine methylation in mammals: who, what, and why. **Mol Cell**. 2009;33:1-13.
21. Wang H, Huang ZQ, Xia L et al. Methylation of histone H4 at arginine 3 facilitating transcriptional activation by nuclear hormone receptor. **Science**. 2001;293:853-857.
22. Huang S, Litt M, Felsenfeld G. Methylation of histone H4 by arginine methyltransferase PRMT1 is essential in vivo for many subsequent histone modifications. **Genes Dev**. 2005;19:1885-1893.
23. An W, Kim J, Roeder RG. Ordered cooperative functions of PRMT1, p300, and CARM1 in transcriptional activation by p53. **Cell**. 2004;117:735-748.
24. Lee DY, Ianculescu I, Purcell D et al. Surface-scanning mutational analysis of protein arginine methyltransferase 1: roles of specific amino acids in methyltransferase substrate specificity, oligomerization, and coactivator function. **Mol Endocrinol**. 2007;21:1381-1393.
25. Lee J, Sayegh J, Daniel J et al. PRMT8, a new membrane-bound tissue-specific member of the protein arginine methyltransferase family. **J Biol Chem**. 2005;280:32890-32896.
26. Bibel M, Richter J, Lacroix E et al. Generation of a defined and uniform population of CNS progenitors and neurons from mouse embryonic stem cells. **Nat Protoc**. 2007;2:1034-1043.
27. Martin B, Bernardon JM, Cavey MT et al. Selective synthetic ligands for human nuclear retinoic acid receptors. **Skin Pharmacol**. 1992;5:57-65.
28. Koszeghy A, Vincze J, Rusznak Z et al. Activation of muscarinic receptors increases the activity of the granule neurones of the rat dorsal cochlear nucleus--a calcium imaging study. **Pflugers Arch**. 2012;463:829-844.
29. Barish GD, Yu RT, Karunasiri MS et al. The Bcl6-SMRT/NCoR cistrome represses inflammation to attenuate atherosclerosis. **Cell Metab**. 2012;15:554-562.
30. Barth L, Sutterlin R, Nenniger M et al. Functional differentiation of stem cell-derived neurons from different murine backgrounds. **Front Cell Neurosci**. 2014;8:49.
31. Niwa H, Miyazaki J, Smith AG. Quantitative expression of Oct-3/4 defines differentiation, dedifferentiation or self-renewal of ES cells. **Nat Genet**. 2000;24:372-376.
32. Diez del Corral R, Storey KG. Markers in vertebrate neurogenesis. **Nat Rev Neurosci**. 2001;2:835-839.
33. Cote J, Boisvert FM, Boulanger MC et al. Sam68 RNA binding protein is an in vivo substrate for protein arginine N-methyltransferase 1. **Mol Biol Cell**. 2003;14:274-287.
34. Sayegh J, Webb K, Cheng D et al. Regulation of protein arginine methyltransferase 8 (PRMT8) activity by its N-terminal domain. **J Biol Chem**. 2007;282:36444-36453.
35. Boisvert FM, Dery U, Masson JY et al. Arginine methylation of MRE11 by PRMT1 is required for DNA damage checkpoint control. **Genes Dev**. 2005;19:671-676.
36. Yu Z, Chen T, Hebert J et al. A mouse PRMT1 null allele defines an essential role for arginine methylation in genome maintenance and cell proliferation. **Mol Cell Biol**. 2009;29:2982-2996.
37. Chevillard-Briet M, Trouche D, Vandel L. Control of CBP co-activating activity by arginine methylation. **EMBO J**. 2002;21:5457-5466.
38. Ceschin DG, Walia M, Wenk SS et al. Methylation specifies distinct estrogen-induced binding site repertoires of CBP to chromatin. **Genes Dev**. 2011;25:1132-1146.
39. Gudas LJ. Retinoids induce stem cell differentiation via epigenetic changes. **Semin Cell Dev Biol**. 2013;24:701-705.

40. Dupe V, Davenne M, Brocard J et al. In vivo functional analysis of the Hoxa-1 3' retinoic acid response element (3'RARE). **Development**. 1997;124:399-410.
41. Ogura T, Evans RM. Evidence for two distinct retinoic acid response pathways for HOXB1 gene regulation. **Proc Natl Acad Sci U S A**. 1995;92:392-396.
42. Kawasaki H, Eckner R, Yao TP et al. Distinct roles of the co-activators p300 and CBP in retinoic-acid-induced F9-cell differentiation. **Nature**. 1998;393:284-289.
43. Kashyap V, Gudas LJ. Epigenetic regulatory mechanisms distinguish retinoic acid-mediated transcriptional responses in stem cells and fibroblasts. **J Biol Chem**. 2010;285:14534-14548.
44. Visel A, Blow MJ, Li Z et al. ChIP-seq accurately predicts tissue-specific activity of enhancers. **Nature**. 2009;457:854-858.
45. Simandi Z, Balint BL, Poliska S et al. Activation of retinoic acid receptor signaling coordinates lineage commitment of spontaneously differentiating mouse embryonic stem cells in embryoid bodies. **FEBS Lett**. 2010;584:3123-3130.
46. Mendoza-Parra MA, Walia M, Sankar M et al. Dissecting the retinoid-induced differentiation of F9 embryonal stem cells by integrative genomics. **Mol Syst Biol**. 2011;7:538.
47. Brunet JF, Pattyn A. Phox2 genes - from patterning to connectivity. **Curr Opin Genet Dev**. 2002;12:435-440.
48. Yoong LF, Too HP. Glial cell line-derived neurotrophic factor and neurturin inhibit neurite outgrowth and activate RhoA through GFR alpha 2b, an alternatively spliced isoform of GFR alpha 2. **J Neurosci**. 2007;27:5603-5614.
49. Helmchen F, Imoto K, Sakmann B. Ca2+ buffering and action potential-evoked Ca2+ signaling in dendrites of pyramidal neurons. **Biophys J**. 1996;70:1069-1081.
50. Stosiek C, Garaschuk O, Holthoff K et al. In vivo two-photon calcium imaging of neuronal networks. **Proc Natl Acad Sci U S A**. 2003;100:7319-7324.
51. Ehtesham M, Thompson RC. CXCR4-Expressing Glial Precursor Cells Demonstrate Enhanced Migratory Tropism for Glioma. **J Cancer Ther**. 2013;3:1086-1091.
52. Idbaih A, Carvalho Silva R, Criniere E et al. Genomic changes in progression of low-grade gliomas. **J Neurooncol**. 2008;90:133-140.
53. Huang J, Vogel G, Yu Z et al. Type II arginine methyltransferase PRMT5 regulates gene expression of inhibitors of differentiation/DNA binding Id2 and Id4 during glial cell differentiation. **J Biol Chem**. 2011;286:44424-44432.
54. Liu Y, Melin BS, Rajaraman P et al. Insight in glioma susceptibility through an analysis of 6p22.3, 12p13.33-12.1, 17q22-23.2 and 18q23 SNP genotypes in familial and non-familial glioma. **Hum Genet**. 2012;131:1507-1517.
55. Kleinschmidt MA, Streubel G, Samans B et al. The protein arginine methyltransferases CARM1 and PRMT1 cooperate in gene regulation. **Nucleic Acids Res**. 2008;36:3202-3213.
56. Lafleur VN, Richard S, Richard DE. Transcriptional repression of hypoxia-inducible factor-1 (HIF-1) by the protein arginine methyltransferase PRMT1. **Mol Biol Cell**. 2014;25:925-935.
57. Rogatsky I, Luecke HF, Leitman DC et al. Alternate surfaces of transcriptional coregulator GRIP1 function in different glucocorticoid receptor activation and repression contexts. **Proc Natl Acad Sci U S A**. 2002;99:16701-16706.
58. Siersbaek R, Nielsen R, John S et al. Extensive chromatin remodelling and establishment of transcription factor 'hotspots' during early adipogenesis. **EMBO J**. 2011;30:1459-1472.

59. Chittka A. Dynamic distribution of histone H4 arginine 3 methylation marks in the developing murine cortex. **PLoS One**. 2010;5:e13807.
60. Baek JH, Rubinstein M, Scheuer T et al. Reciprocal Changes in Phosphorylation and Methylation of Mammalian Brain Sodium Channels in Response to Seizures. **J Biol Chem**. 2014;289:15363-15373.
61. Lee HP, Casadesus G, Zhu X et al. All-trans retinoic acid as a novel therapeutic strategy for Alzheimer's disease. **Expert Rev Neurother**. 2009;9:1615-1621.
62. Miller JA, Woltjer RL, Goodenbour JM et al. Genes and pathways underlying regional and cell type changes in Alzheimer's disease. **Genome Med**. 2013;5:48.
63. Lin YL, Tsai YJ, Liu YF et al. The Critical Role of Protein Arginine Methyltransferase prmt8 in Zebrafish Embryonic and Neural Development Is Non-Redundant with Its Paralogue prmt1. **PLoS One**. 2013;8:e55221.
64. Ali R, Campos B, Dyckhoff G et al. Quantification of retinoid concentrations in human serum and brain tumor tissues. **Anal Chim Acta**. 2012;725:57-66.
65. Wang S, Tan X, Yang B et al. The role of protein arginine-methyltransferase 1 in gliomagenesis. **BMB Rep**. 2012;45:470-475.
66. Kousaka A, Mori Y, Koyama Y et al. The distribution and characterization of endogenous protein arginine N-methyltransferase 8 in mouse CNS. **Neuroscience**. 2009;163:1146-1157.
67. Hu B, Thirtamara-Rajamani KK, Sim H et al. Fibulin-3 is uniquely upregulated in malignant gliomas and promotes tumor cell motility and invasion. **Mol Cancer Res**. 2009;7:1756-1770.
68. do Carmo A, Patricio I, Cruz MT et al. CXCL12/CXCR4 promotes motility and proliferation of glioma cells. **Cancer Biol Ther**. 2010;9:56-65.

**Figure 1.**

Simandi et al. (Nagy)

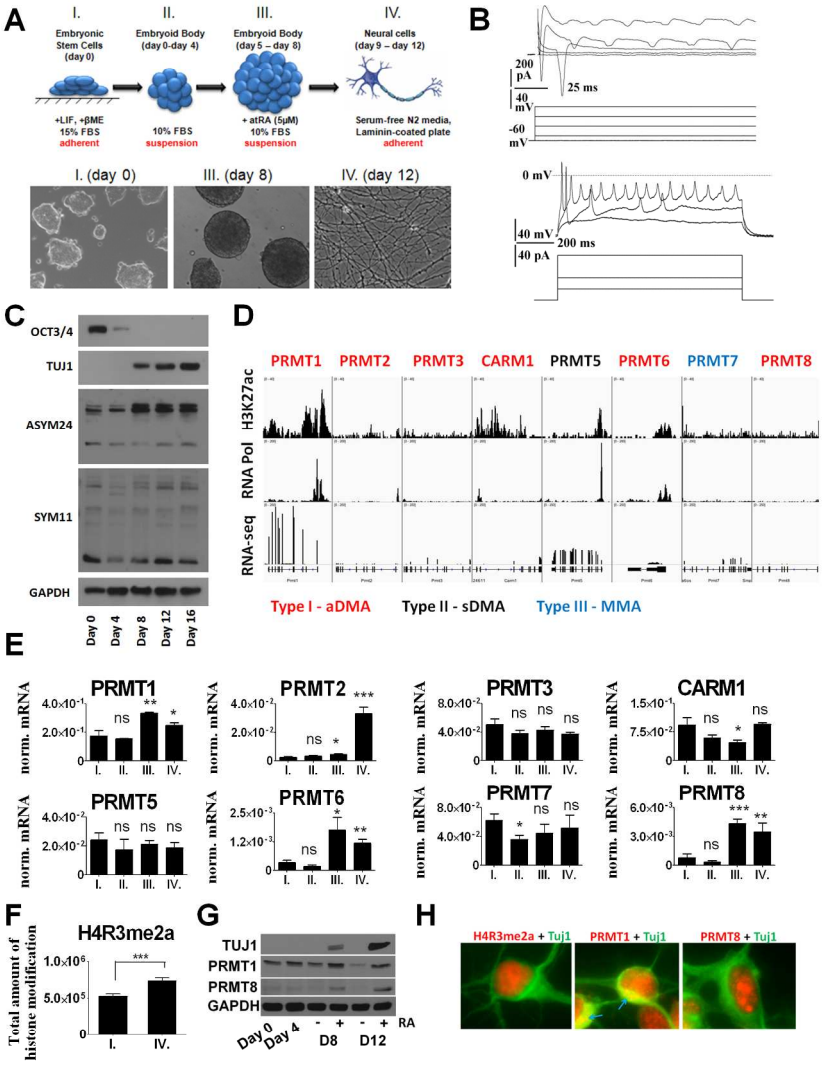


190x274mm (284 x 284 DPI)

**Figure 2.**

Simandi et al. (Nagy)

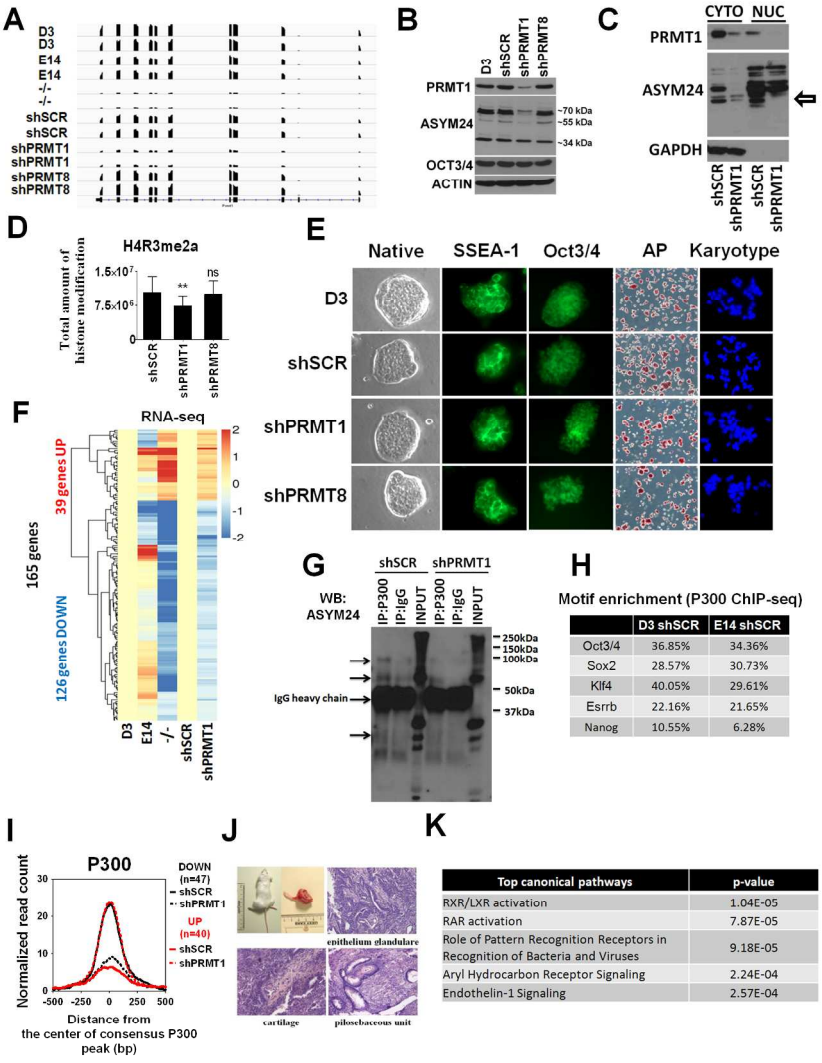


| | D3 shSCR | E14 shSCR |
|---|---|---|
| Oct3/4 | 36.85% | 34.36% |
| Sox2 | 28.57% | 30.73% |
| Klf4 | 40.05% | 29.61% |
| Esrrb | 22.16% | 21.65% |
| Nanog | 10.55% | 6.28% |

| Top canonical pathways | p-value |
|---|---|
| RXR/LXR activation | 1.04E-05 |
| RAR activation | 7.87E-05 |
| Role of Pattern Recognition Receptors in Recognition of Bacteria and Viruses | 9.18E-05 |
| Aryl Hydrocarbon Receptor Signaling | 2.24E-04 |
| Endothelin-1 Signaling | 2.57E-04 |

190x274mm (284 x 284 DPI)

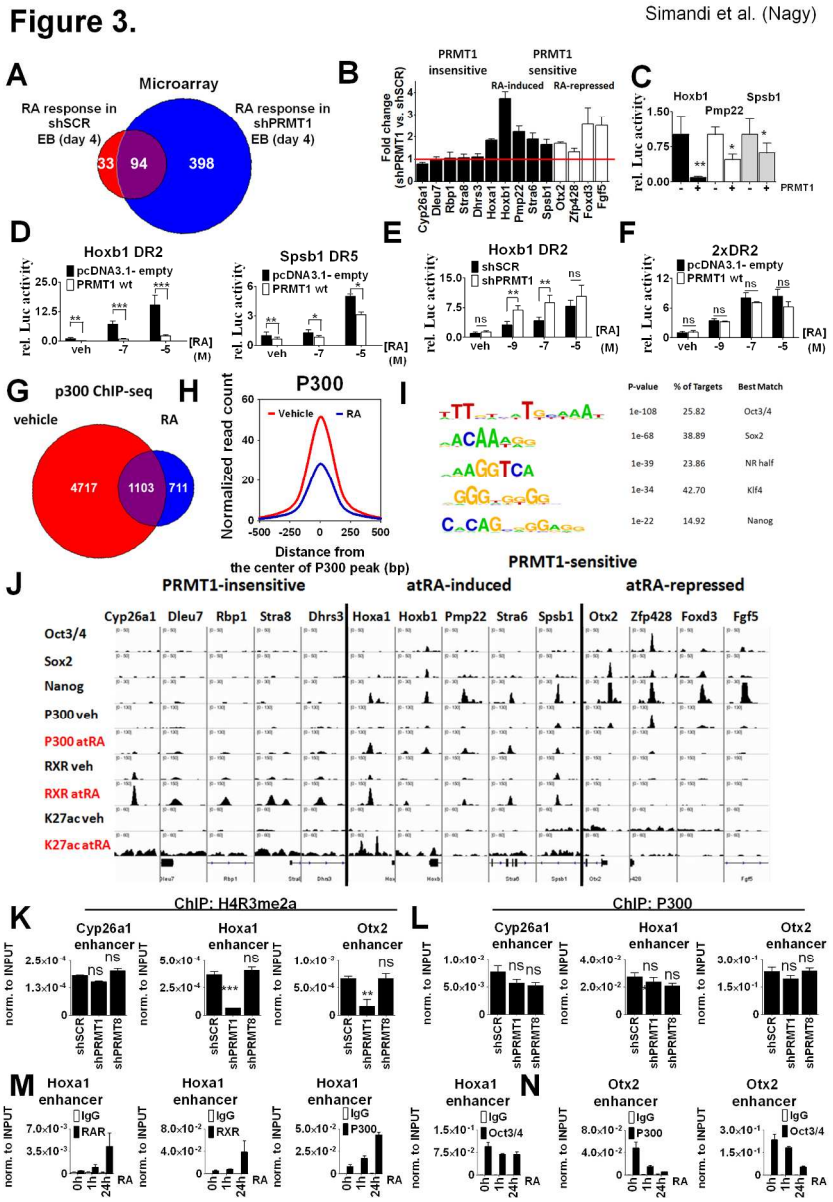


190x274mm (284 x 284 DPI)

**Figure 4.**

Simandi et al. (Nagy)

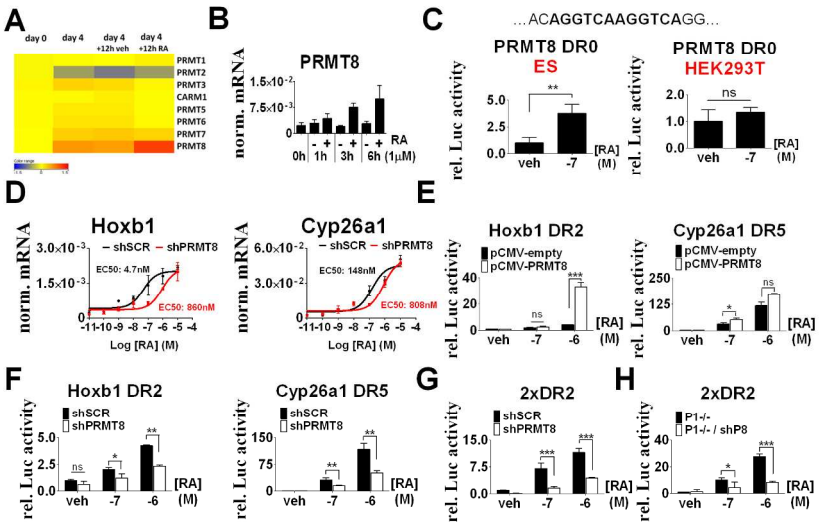


190x274mm (284 x 284 DPI)

**Figure 5.**

Simandi et al. (Nagy)

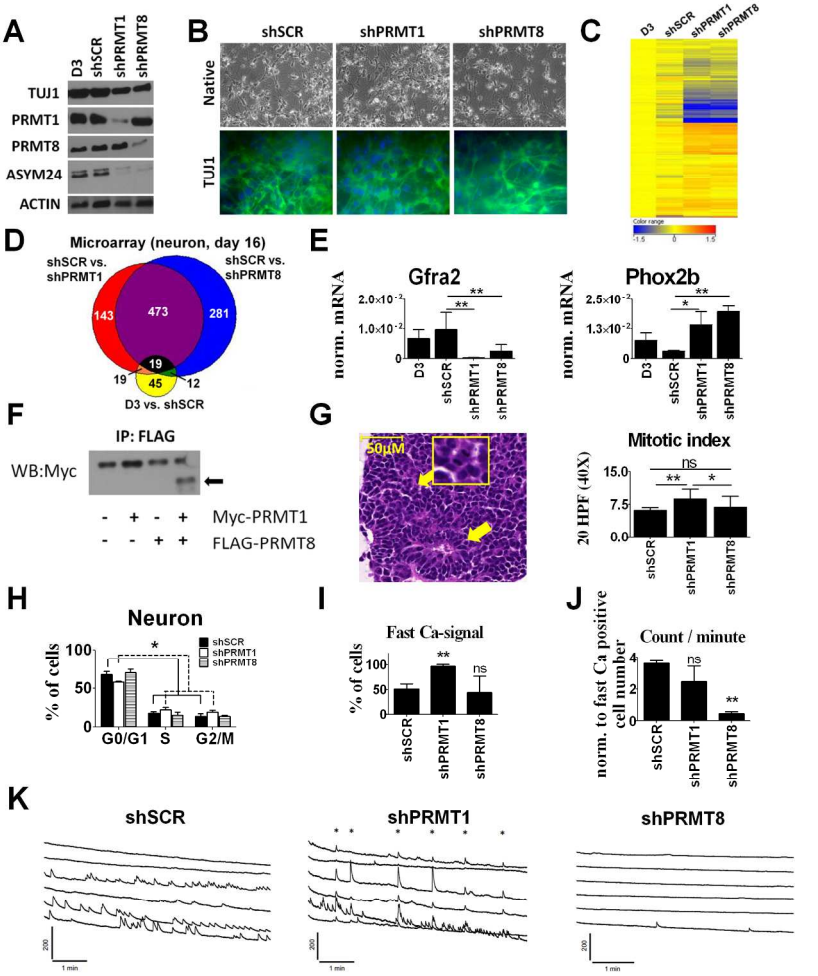


190x274mm (284 x 284 DPI)

**Figure 6.**

Simandi et al. (Nagy)

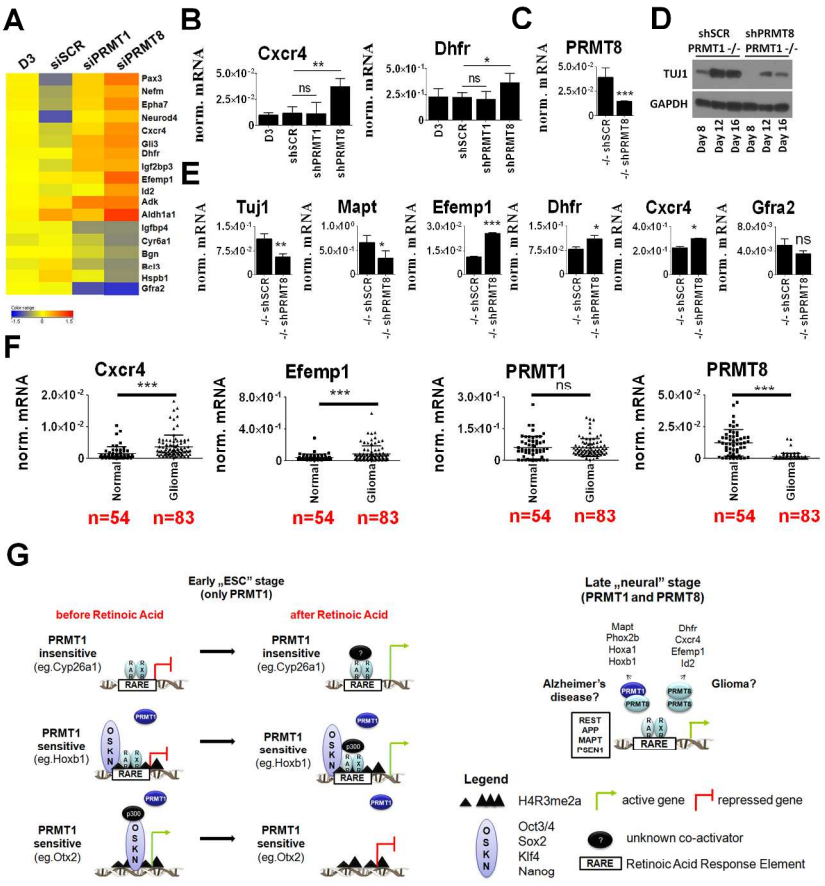


190x274mm (284 x 284 DPI)

**Figure S1.**

Simandi et al. (Nagy)

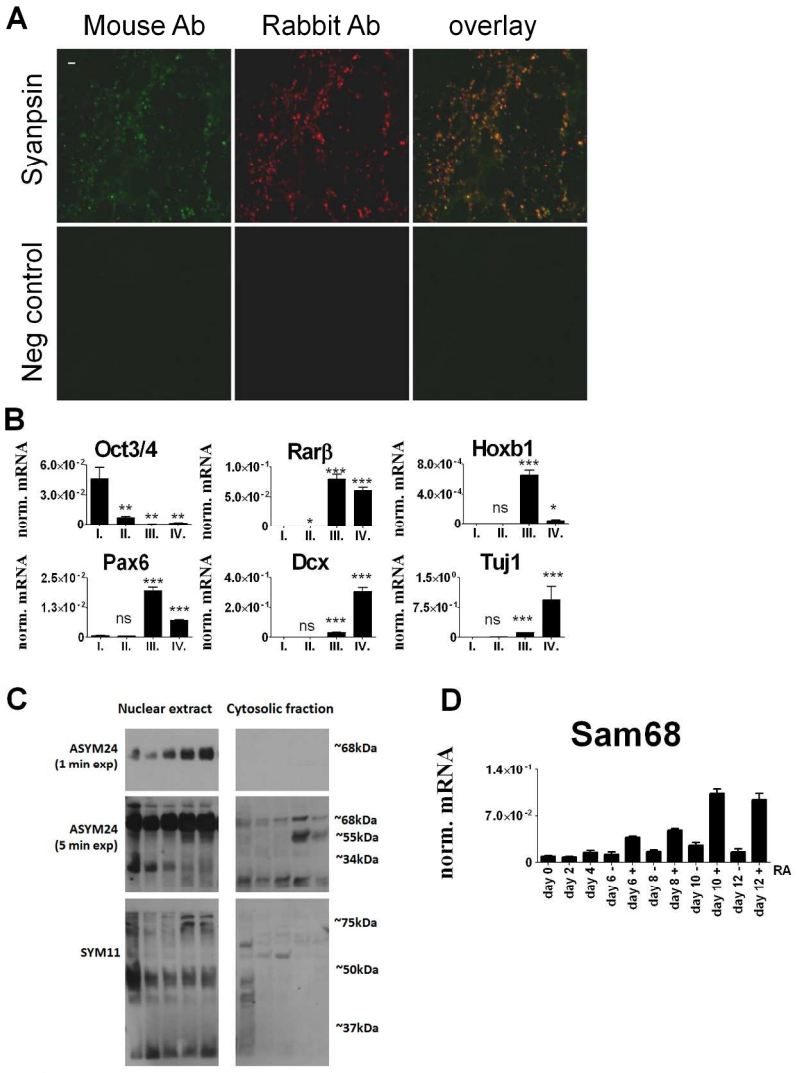


190x274mm (284 x 284 DPI)

**Figure S2.**

Simandi et al. (Nagy)

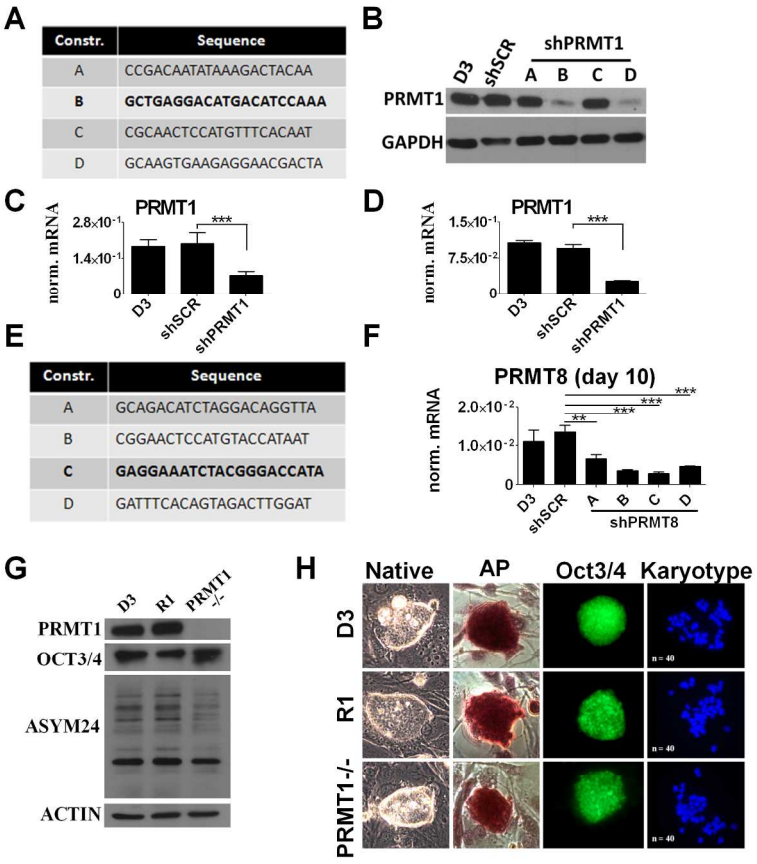


190x274mm (284 x 284 DPI)

**Figure S3.**

Simandi et al. (Nagy)

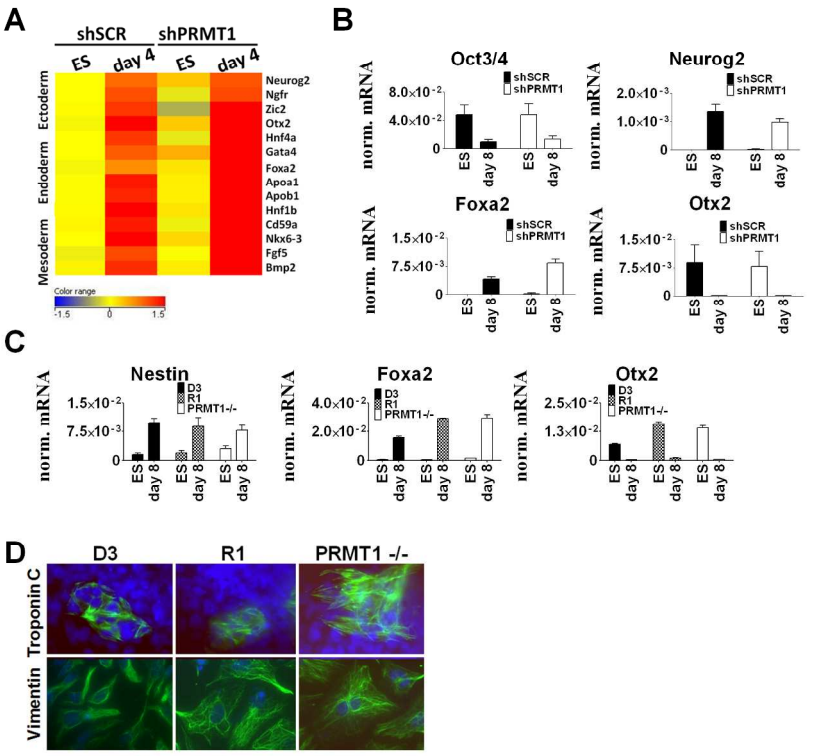


190x274mm (284 x 284 DPI)

**Figure S4.**

Simandi et al. (Nagy)

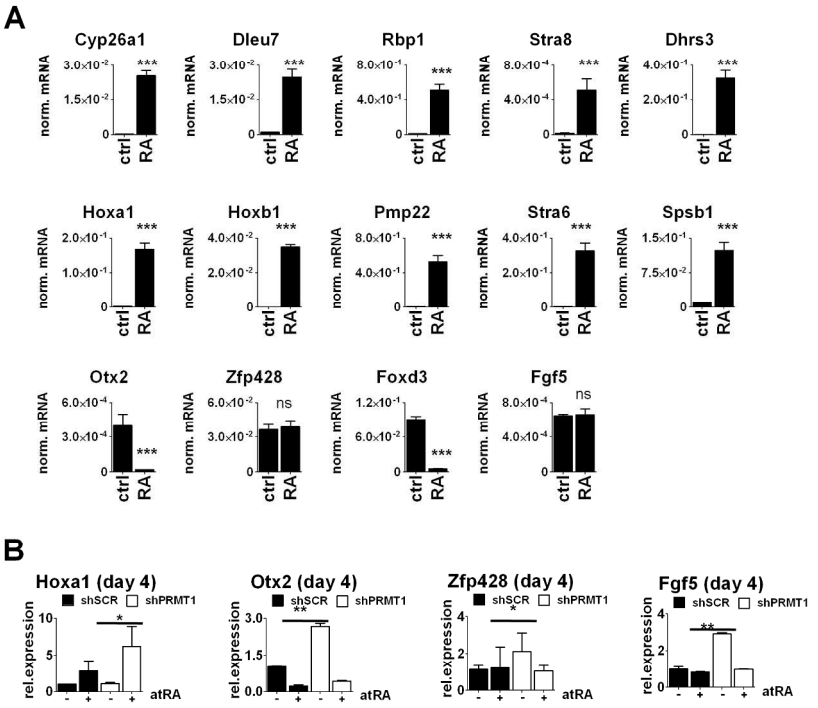


190x274mm (284 x 284 DPI)

**Figure S5.**

Simandi et al. (Nagy)

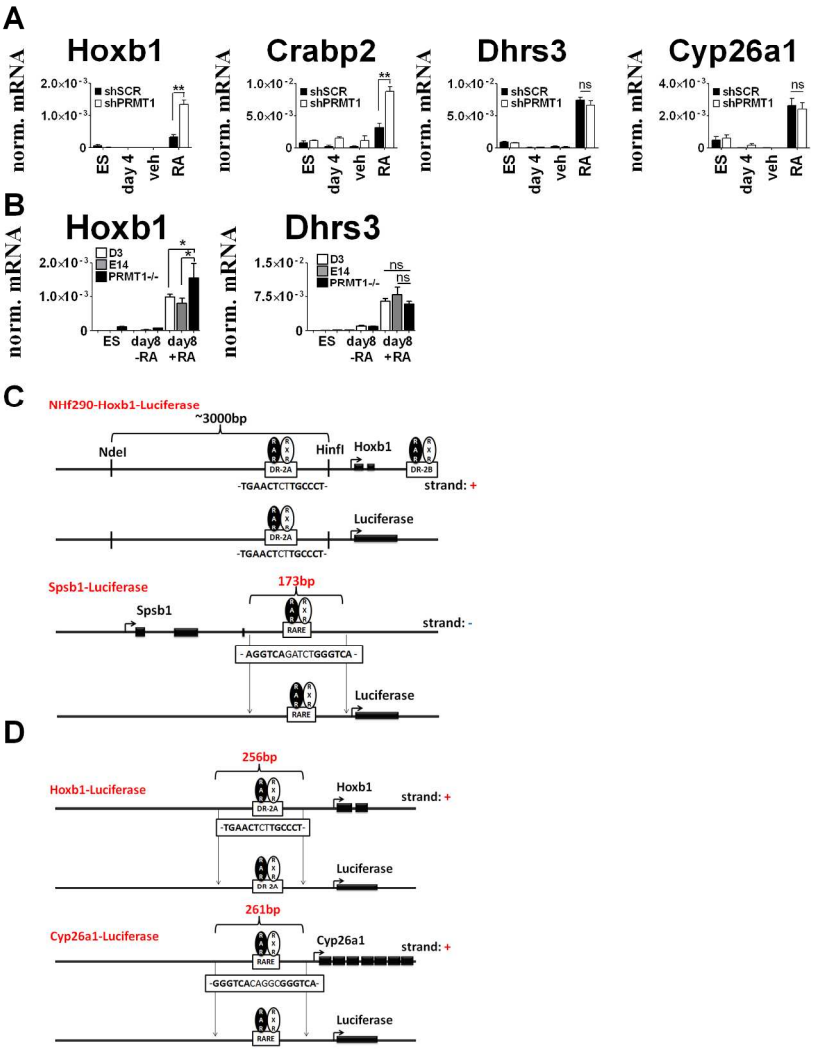


190x274mm (284 x 284 DPI)

**Figure S6.**

Simandi et al. (Nagy)

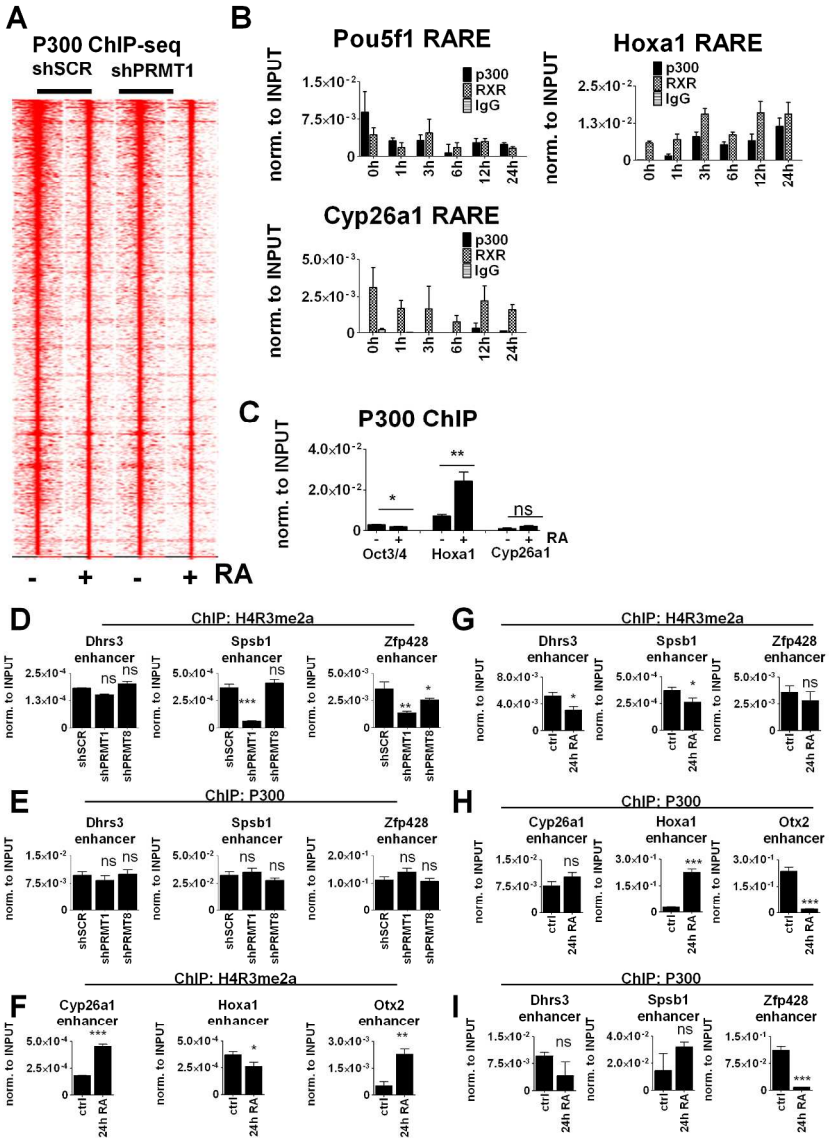


190x274mm (284 x 284 DPI)

**Figure S7.**

Simandi et al. (Nagy)

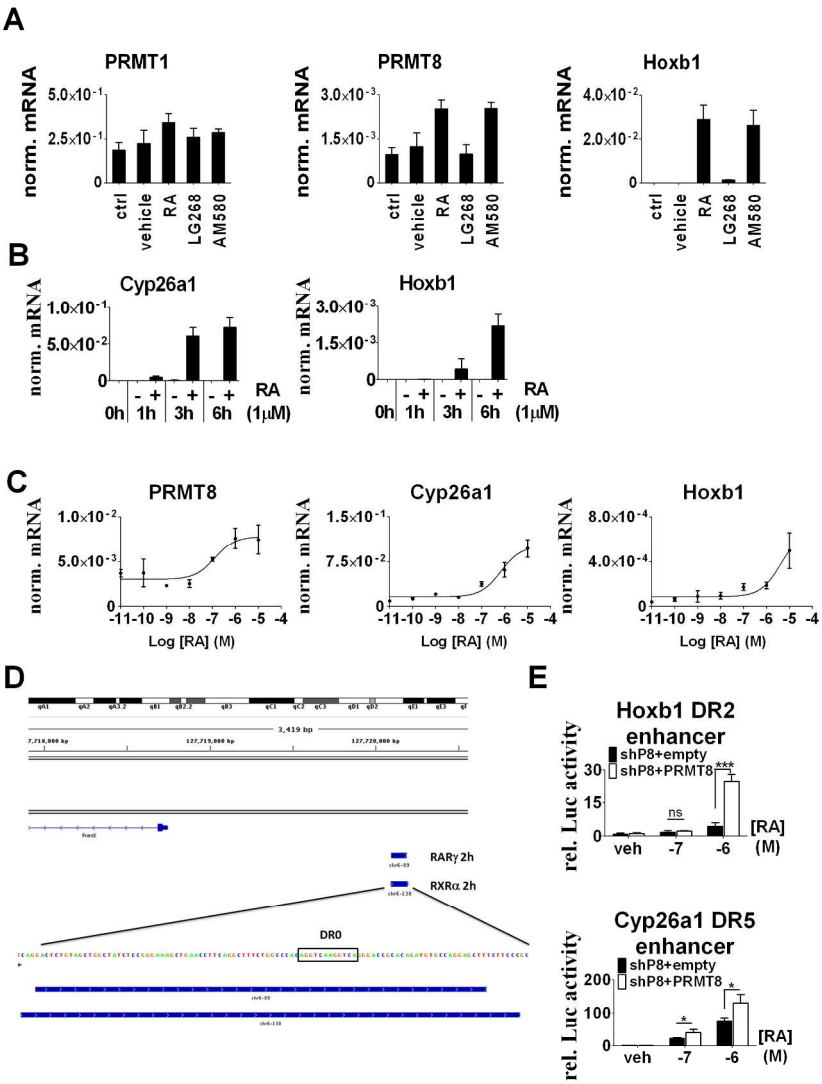


190x274mm (284 x 284 DPI)

**Figure S8.**

Simandi et al. (Nagy)

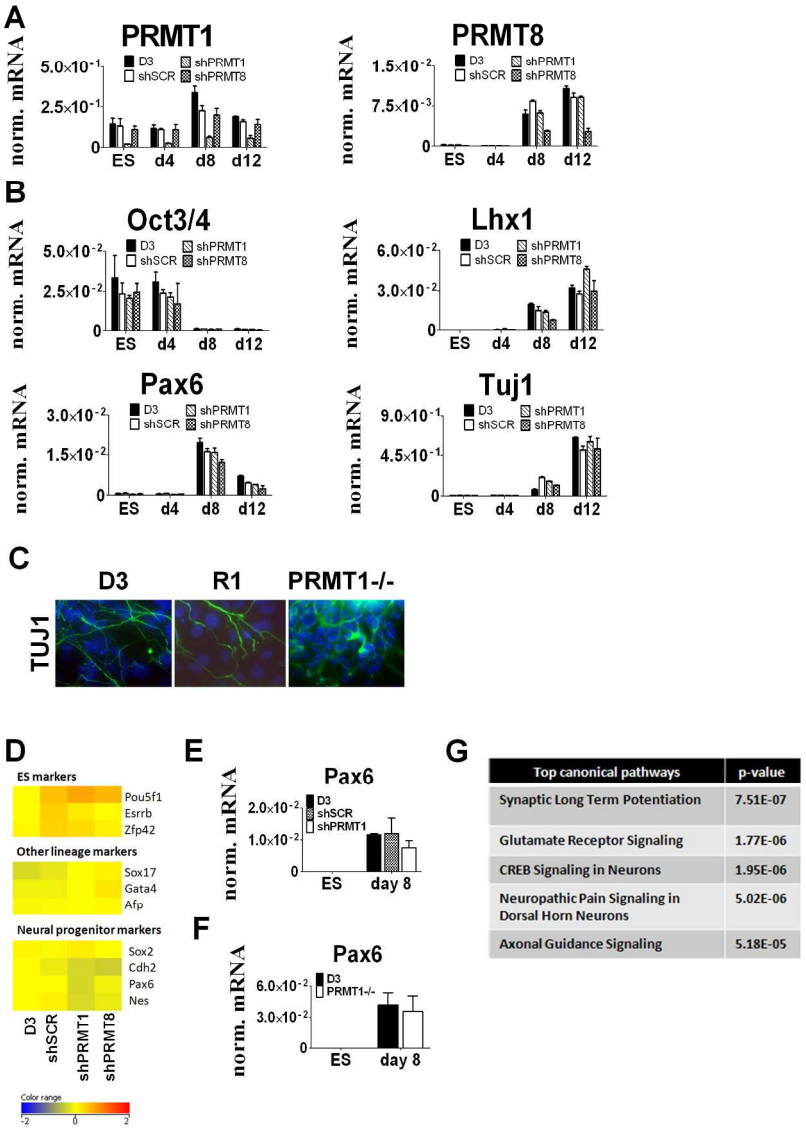


| Top canonical pathways | p-value |
|---|---|
| Synaptic Long Term Potentiation | 7.51E-07 |
| Glutamate Receptor Signaling | 1.77E-06 |
| CREB Signaling in Neurons | 1.95E-06 |
| Neuropathic Pain Signaling in Dorsal Horn Neurons | 5.02E-06 |
| Axonal Guidance Signaling | 5.18E-05 |

190x274mm (284 x 284 DPI)

**Figure S9.**

Simandi et al. (Nagy)

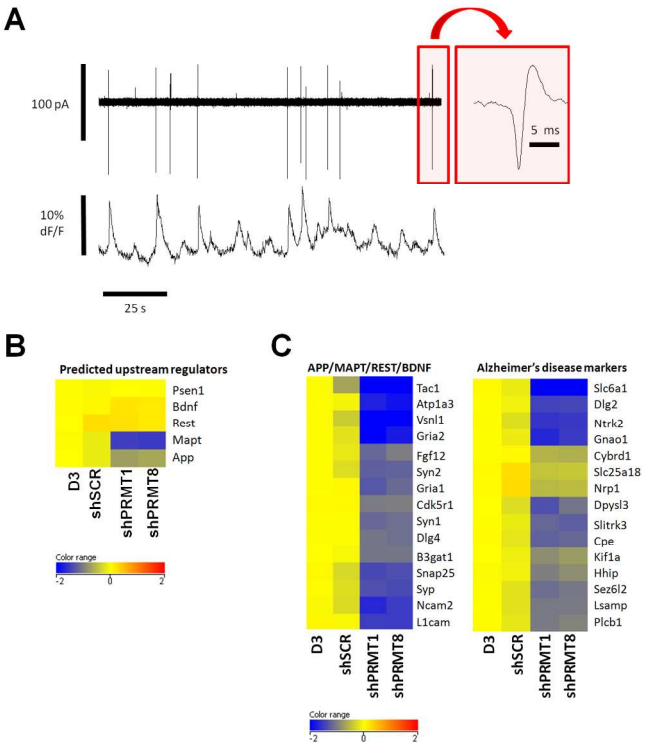


190x274mm (284 x 284 DPI)

| Gene | Location | PRMT1 KO vs D3 | | PRMT1 KO vs E14 | | shPRMT1 vs shSCR | |
|---|---|---|---|---|---|---|---|
| | | log2FC | p-value | log2FC | p-value | log2FC | p-value |
| 1700030C10Rik | chr12:20810252-20821640 | 1.83372 | 5.00E-05 | 2.28297 | 5.00E-05 | 1.08975 | 5.00E-05 |
| 2310046K01Rik | chr2:151822246-151834994 | 1.02763 | 5.00E-05 | 1.9927 | 5.00E-05 | 0.649408 | 0.00025 |
| 2610002M06Rik | chrX:104978090-105011673 | -1.25181 | 5.00E-05 | -0.71153 | 5.00E-05 | -0.52773 | 8.00E-04 |
| 2900011O08Rik | chr16:13986729-14101587 | -1.43578 | 5.00E-05 | -1.77644 | 5.00E-05 | -0.62182 | 3.00E-04 |
| 6230409E13Rik | chr4:21858472-21928608 | -0.999754 | 5.00E-05 | -1.33394 | 5.00E-05 | -0.71506 | 5.00E-05 |
| 9130008F23Rik | chr17:41012430-41017507 | -3.86922 | 0.00075 | -2.62254 | 0.00515 | -1.49854 | 0.00025 |
| Aass | chr6:23022172-23082986 | -2.00649 | 5.00E-05 | -2.53942 | 5.00E-05 | -0.56045 | 0.00025 |
| Acta2 | chr19:34315580-34329826 | -7.32174 | 0.00075 | -10.3179 | 0.00075 | -0.80701 | 1.00E-04 |
| Adamts1 | chr16:85794072-85803360 | -3.80065 | 5.00E-05 | -3.79962 | 5.00E-05 | -1.25657 | 5.00E-05 |
| Aes | chr10:81022304-81029109 | 1.20724 | 5.00E-05 | 0.443892 | 0.0016 | 0.490396 | 0.00035 |
| Ahr | chr12:36182650-36219661 | -0.733575 | 5.00E-05 | -1.06212 | 5.00E-05 | -0.55653 | 9.00E-04 |
| AI662270 | chr11:83037077-83040086 | -1.19181 | 5.00E-05 | -1.05957 | 5.00E-05 | -0.93374 | 5.00E-05 |
| Aim1 | chr10:43670112-43724652 | -1.88033 | 5.00E-05 | -1.60654 | 5.00E-05 | -0.71313 | 0.0012 |
| Ankrd1 | chr19:36186454-36194334 | -0.866334 | 0.01015 | -3.24372 | 5.00E-05 | -1.53165 | 2.00E-04 |
| Ankrd35 | chr3:96474053-96494957 | 1.86417 | 5.00E-05 | 0.842451 | 5.00E-05 | 0.573932 | 9.00E-04 |
| Anxa1 | chr19:20447923-20465161 | -4.14478 | 5.00E-05 | -4.73546 | 5.00E-05 | -0.58817 | 8.00E-04 |
| Anxa3 | chr5:97222403-97274987 | -1.412 | 5.00E-05 | -1.36884 | 5.00E-05 | -0.71337 | 1.00E-04 |
| Atp10a | chr7:65913571-66084796 | -3.33172 | 5.00E-05 | -3.47959 | 5.00E-05 | -0.86429 | 5.00E-05 |
| Atp2a3 | chr11:72774670-72806545 | 1.74777 | 5.00E-05 | 2.36242 | 5.00E-05 | 0.661102 | 5.00E-05 |
| AW551984 | chr9:39394980-39411709 | -1.14325 | 5.00E-05 | -1.66055 | 5.00E-05 | -0.64955 | 0.00025 |
| Bche | chr3:73439730-73512337 | -3.22899 | 5.00E-05 | -2.00731 | 5.00E-05 | -0.64838 | 0.00095 |
| Calcr | chr6:3635719-3714713 | -2.92656 | 5.00E-05 | -1.86029 | 1.00E-04 | -1.30968 | 5.00E-05 |
| Camk2n1 | chr4:138011062-138016041 | 4.17485 | 5.00E-05 | 1.24493 | 5.00E-05 | 0.818474 | 5.00E-05 |
| Car2 | chr3:14886425-14900770 | -2.49805 | 5.00E-05 | -2.23579 | 5.00E-05 | -0.81198 | 5.00E-05 |
| Ccdc85a | chr11:28285691-28484296 | -2.64409 | 5.00E-05 | -0.82887 | 0.00065 | -0.61651 | 1.00E-04 |
| Cd59a | chr2:103935957-103955508 | -2.22883 | 5.00E-05 | -1.13626 | 5.00E-05 | -0.65355 | 3.00E-04 |
| Cdh2 | chr18:16747385-16967558 | -4.90404 | 5.00E-05 | -4.24413 | 5.00E-05 | -0.68073 | 5.00E-05 |
| Cdk14 | chr5:4803384-5380251 | -1.54955 | 5.00E-05 | -1.07496 | 5.00E-05 | -0.81221 | 3.00E-04 |
| Chrdl1 | chrX:139720216-139828805 | -2.75647 | 5.00E-05 | -2.90885 | 5.00E-05 | -1.17149 | 2.00E-04 |
| Chst1 | chr2:92439863-92455409 | -1.23383 | 0.00125 | -2.1473 | 5.00E-05 | -0.76301 | 1.00E-04 |
| Chst15 | chr7:139427937-139509974 | -0.724828 | 5.00E-05 | -1.03064 | 5.00E-05 | -1.15243 | 5.00E-05 |
| Cldn7 | chr11:69778280-69781388 | -0.813758 | 5.00E-05 | -0.63703 | 1.00E-04 | -0.57245 | 1.00E-04 |
| Clvs2 | chr10:33232139-33344406 | -3.84228 | 5.00E-05 | -2.86465 | 5.00E-05 | -1.1861 | 5.00E-05 |
| Col1a2 | chr6:4455696-4491543 | -3.94804 | 5.00E-05 | -9.66705 | 5.00E-05 | -0.82387 | 1.00E-04 |
| Col5a2 | chr1:45431175-45560127 | -3.34171 | 5.00E-05 | -4.02944 | 5.00E-05 | -0.97221 | 5.00E-05 |
| Colec12 | chr18:9707645-9877993 | -2.14771 | 5.00E-05 | -1.5118 | 5.00E-05 | -0.8756 | 5.00E-05 |
| Cpeb1 | chr7:88491911-88599644 | -0.536218 | 0.0015 | -1.75171 | 5.00E-05 | -0.58583 | 3.00E-04 |
| Crispld1 | chr1:17717497-17756288 | -3.42753 | 5.00E-05 | -1.92292 | 5.00E-05 | -1.21302 | 5.00E-05 |
| Csf1 | chr3:107543965-107563387 | -2.71659 | 5.00E-05 | -4.20064 | 5.00E-05 | -0.90157 | 9.00E-04 |

| | | | | | | | |
|---|---|---|---|---|---|---|---|
| Ctgf | chr10:24315247-24318488 | -2.50087 | 5.00E-05 | -2.54953 | 5.00E-05 | -1.13214 | 5.00E-05 |
| Cthrc1 | chr15:38908477-38918665 | -0.75674 | 1.00E-04 | -0.74237 | 2.00E-04 | -0.84097 | 5.00E-05 |
| Cubn | chr2:13197964-13413503 | 0.34178 | 0.01355 | 1.37041 | 5.00E-05 | 0.461708 | 0.0013 |
| Cyr61 | chr3:145309934-145312949 | -2.3809 | 5.00E-05 | -2.46991 | 5.00E-05 | -1.1706 | 5.00E-05 |
| Dcaf12l1 | chrX:42139743-42143374 | -1.19862 | 5.00E-05 | -0.73228 | 5.00E-05 | -0.81278 | 5.00E-05 |
| Ddx3y | chrY:597157-623056 | -1.32685 | 5.00E-05 | -2.31784 | 5.00E-05 | -0.85324 | 0.00035 |
| Dnaja4 | chr9:54547365-54564124 | -1.88232 | 5.00E-05 | -1.79913 | 5.00E-05 | -0.65074 | 1.00E-04 |
| Dppa3 | chr6:122576441-122580289 | -0.899457 | 5.00E-05 | -2.97794 | 5.00E-05 | -0.99738 | 5.00E-05 |
| Dtx4 | chr19:12540825-12576486 | -1.60719 | 5.00E-05 | -2.10655 | 5.00E-05 | -0.86347 | 5.00E-05 |
| Eif5a2 | chr3:28680232-28697768 | -0.728228 | 5.00E-05 | -0.47744 | 0.00165 | -0.46814 | 0.00095 |
| Elmo1 | chr13:20182375-20700222 | -0.665753 | 5.00E-05 | -0.62048 | 1.00E-04 | -0.57477 | 0.00015 |
| Enpp2 | chr15:54670452-54751701 | -5.29971 | 5.00E-05 | -1.92725 | 5.00E-05 | -0.93937 | 5.00E-05 |
| Erap1 | chr13:74777319-74829323 | -2.14088 | 5.00E-05 | -0.82456 | 5.00E-05 | -0.62681 | 6.00E-04 |
| Etv4 | chr11:101631055-101646624 | 1.17857 | 5.00E-05 | 2.21751 | 5.00E-05 | 0.68176 | 5.00E-05 |
| Fam102b | chr3:108773914-108830525 | -0.520599 | 0.00165 | -1.60277 | 5.00E-05 | -0.5144 | 0.00125 |
| Fam120c | chrX:147778765-147908677 | 1.2379 | 5.00E-05 | 0.534974 | 0.00085 | 0.701652 | 3.00E-04 |
| Fam46a | chr9:85214045-85220757 | -1.46585 | 5.00E-05 | -1.00874 | 5.00E-05 | -0.60492 | 3.00E-04 |
| Fgf13 | chrX:56315327-56387613 | -1.93367 | 5.00E-05 | -1.81784 | 5.00E-05 | -0.74374 | 1.00E-04 |
| Fgfbp1 | chr5:44370098-44373001 | -3.90251 | 5.00E-05 | -1.86958 | 5.00E-05 | -1.09523 | 5.00E-05 |
| Fgfr2 | chr7:137305964-137410322 | -0.834932 | 5.00E-05 | -1.05924 | 5.00E-05 | -0.51254 | 0.00065 |
| Fndc3c1 | chrX:103615381-103680568 | -4.52857 | 5.00E-05 | -3.79785 | 5.00E-05 | -0.81795 | 5.00E-05 |
| Frem2 | chr3:53317859-53461277 | -1.45557 | 5.00E-05 | -1.86431 | 5.00E-05 | -0.52122 | 0.00025 |
| Gab2 | chr7:104230260-104457461 | -1.40682 | 5.00E-05 | -2.46838 | 5.00E-05 | -0.71212 | 0.001 |
| Gad1 | chr2:70327996-70440069 | -1.52569 | 5.00E-05 | -2.03477 | 5.00E-05 | -0.56107 | 2.00E-04 |
| Gbp1 | chr3:142257810-142282140 | -4.99914 | 5.00E-05 | -4.81088 | 5.00E-05 | -1.03337 | 5.00E-05 |
| Gbp2 | chr3:142283626-142300972 | -4.29012 | 5.00E-05 | -4.27035 | 5.00E-05 | -0.87053 | 5.00E-05 |
| Gbp3 | chr3:142223015-142236176 | -5.40262 | 5.00E-04 | -4.92103 | 5.00E-04 | -1.03504 | 0.00015 |
| Gbp7 | chr3:142193301-142213047 | -3.60664 | 5.00E-05 | -4.17095 | 5.00E-05 | -0.90663 | 5.00E-05 |
| Gm13251 | chr4:145728598-145749009 | 1.20067 | 5.00E-05 | 2.54502 | 5.00E-05 | 1.10747 | 5.00E-05 |
| Gm7325 | chr17:45737915-45739051 | 0.593475 | 0.00015 | 1.87248 | 5.00E-05 | 0.970834 | 5.00E-05 |
| Gm8615 | chr5:149931140-149993612 | 0.573727 | 0.00015 | 0.471491 | 0.0021 | 0.492085 | 0.00095 |
| Gna14 | chr19:16510156-16685308 | -0.889821 | 5.00E-05 | -0.92787 | 5.00E-05 | -0.8288 | 1.00E-04 |
| Gpm6b | chrX:162676874-162826965 | -1.16954 | 5.00E-05 | -0.71357 | 0.00445 | -0.9757 | 1.00E-04 |
| Gramd1c | chr16:43980462-44028058 | -1.76733 | 5.00E-05 | -1.32769 | 5.00E-05 | -0.85265 | 0.00045 |
| H19 | chr7:149761436-149764051 | -2.21183 | 5.00E-05 | -1.74644 | 5.00E-05 | -1.06596 | 5.00E-05 |
| Has2 | chr15:56497181-56526101 | -2.56874 | 5.00E-05 | -1.90017 | 5.00E-05 | -0.62228 | 6.00E-04 |
| Hdac1 | chr4:129193347-129219890 | 1.78895 | 5.00E-05 | 2.35874 | 5.00E-05 | 0.762522 | 0.00025 |
| Hmga2 | chr10:119798330-119913991 | -0.813537 | 5.00E-05 | -1.64483 | 5.00E-05 | -0.59619 | 0.00045 |
| Hmgn3 | chr9:83003548-83040214 | -2.51204 | 5.00E-05 | -2.1834 | 5.00E-05 | -0.59777 | 0.0011 |
| Hspa8 | chr9:40609355-40613282 | 0.742855 | 5.00E-05 | 0.519679 | 2.00E-04 | 0.715594 | 5.00E-05 |
| Hspb1 | chr5:136363788-136365433 | 0.800543 | 5.00E-05 | 0.817489 | 5.00E-05 | 1.02759 | 5.00E-05 |

| | | | | | | | |
|---|---|---|---|---|---|---|---|
| Id2 | chr12:25778663-25780957 | -1.63996 | 5.00E-05 | -1.13785 | 5.00E-05 | -0.78226 | 5.00E-05 |
| Igfbp3 | chr11:7106095-7113926 | -2.09348 | 5.00E-05 | -1.964 | 5.00E-05 | -0.76508 | 5.00E-05 |
| Igsf11 | chr16:38902457-39027270 | -1.99499 | 5.00E-05 | -2.24447 | 5.00E-05 | -0.83717 | 5.00E-05 |
| Igsf21 | chr4:139582766-139802726 | 2.73105 | 5.00E-05 | 1.95693 | 5.00E-05 | 0.840501 | 5.00E-05 |
| Inhbb | chr1:121312041-121318825 | 0.997349 | 5.00E-05 | 2.65833 | 5.00E-05 | 0.591109 | 5.00E-05 |
| Irs1 | chr1:82229679-82288014 | -2.83759 | 5.00E-05 | -3.64504 | 5.00E-05 | -0.74025 | 5.00E-05 |
| Jph1 | chr1:16985020-17087970 | -1.89612 | 5.00E-05 | -1.57162 | 5.00E-05 | -0.61068 | 4.00E-04 |
| Kcnj3 | chr2:55289566-55447936 | -5.88978 | 5.00E-05 | -3.39887 | 5.00E-05 | -0.76117 | 5.00E-05 |
| Kcnk1 | chr8:128519001-128554585 | -0.700896 | 5.00E-05 | -0.59184 | 1.00E-04 | -0.57311 | 0.00035 |
| Kctd12b | chrX:150119696-150130823 | -3.21317 | 5.00E-05 | -2.31653 | 5.00E-05 | -1.84932 | 5.00E-05 |
| Kif1a | chr1:94912032-94998442 | -1.78213 | 5.00E-05 | -2.94451 | 5.00E-05 | -0.72651 | 5.00E-05 |
| Klf6 | chr13:5860734-5869639 | -1.06601 | 5.00E-05 | -1.038 | 5.00E-05 | -0.50887 | 2.00E-04 |
| Krt19 | chr11:100002125-100007233 | -1.07321 | 5.00E-05 | -1.18812 | 5.00E-05 | -0.64269 | 5.00E-05 |
| Lama4 | chr10:38685320-38829994 | -2.08813 | 5.00E-05 | -2.61885 | 5.00E-05 | -0.75846 | 0.0013 |
| Lpl | chr8:71404453-71430831 | -1.32872 | 5.00E-05 | -1.67174 | 5.00E-05 | -0.7298 | 5.00E-05 |
| Mal2 | chr15:54402920-54434401 | -1.26894 | 5.00E-05 | -0.92199 | 5.00E-05 | -0.62483 | 9.00E-04 |
| Mapt | chr11:104092749-104193407 | 2.84632 | 5.00E-05 | 2.73179 | 5.00E-05 | 0.754977 | 5.00E-05 |
| Mcf2 | chrX:57309132-57400820 | 0.968176 | 5.00E-05 | 1.21632 | 5.00E-05 | 0.874408 | 1.00E-04 |
| Mcoln3 | chr3:145784754-145803610 | -1.55308 | 0.00035 | -2.21241 | 5.00E-05 | -0.96224 | 5.00E-05 |
| Mfap3l | chr8:63111656-63155528 | -1.21868 | 5.00E-05 | -1.55394 | 5.00E-05 | -0.83347 | 5.00E-05 |
| Mgst1 | chr6:138089057-138105273 | -1.2109 | 5.00E-05 | -1.61203 | 5.00E-05 | -0.71538 | 5.00E-05 |
| Mlf1 | chr3:67178018-67203922 | -1.17853 | 5.00E-05 | -1.48939 | 5.00E-05 | -0.66325 | 2.00E-04 |
| Myl9 | chr2:156601199-156607393 | -4.24239 | 5.00E-05 | -4.7499 | 5.00E-05 | -0.94502 | 7.00E-04 |
| Ncoa4 | chr14:32973077-32992549 | 2.82582 | 5.00E-05 | 2.09691 | 5.00E-05 | 0.997778 | 0.0011 |
| Nes | chr3:87775014-87784373 | -3.16089 | 5.00E-05 | -2.56683 | 5.00E-05 | -1.0488 | 5.00E-05 |
| Pax6 | chr2:105376236-105537521 | -3.21451 | 5.00E-05 | -3.0544 | 5.00E-05 | -0.80191 | 0.001 |
| Pcsk1 | chr13:75227434-75269946 | -1.54216 | 5.00E-05 | -1.43255 | 5.00E-05 | -0.7224 | 0.001 |
| Pde9a | chr17:31523178-31613254 | 2.53226 | 5.00E-05 | 1.84753 | 5.00E-05 | 0.632934 | 8.00E-04 |
| Pdgfa | chr5:139452928-139470907 | 1.17407 | 5.00E-05 | 1.20029 | 5.00E-05 | 0.785688 | 5.00E-05 |
| Pdlim3 | chr8:46970838-47004900 | -1.31697 | 0.0015 | -4.17517 | 5.00E-05 | -0.98907 | 5.00E-05 |
| Penk | chr4:4060682-4065592 | -2.49441 | 5.00E-05 | -2.22269 | 5.00E-05 | -0.77443 | 0.00015 |
| Pion | chr5:20692084-20797519 | -1.13982 | 2.00E-04 | -2.69632 | 5.00E-05 | -1.08871 | 5.00E-05 |
| Pkia | chr3:7366603-7445365 | -2.1954 | 5.00E-05 | -1.33577 | 5.00E-05 | -0.97775 | 5.00E-05 |
| Pla2g4a | chr1:151676751-151808414 | -2.4174 | 5.00E-05 | -2.47701 | 5.00E-05 | -0.86973 | 5.00E-05 |
| Pm20d2 | chr4:33257381-33276712 | -1.48276 | 5.00E-05 | -1.51768 | 5.00E-05 | -0.63003 | 5.00E-05 |
| Pof1b | chrX:109752035-109812260 | -3.48979 | 5.00E-05 | -3.08002 | 5.00E-05 | -0.90324 | 5.00E-04 |
| Polr3gl | chr3:96381796-96398081 | 1.17243 | 5.00E-05 | 2.22132 | 5.00E-05 | 0.781693 | 5.00E-05 |
| Prmt1 | chr7:52232124-52241790 | -3.22664 | 5.00E-05 | -2.42597 | 5.00E-05 | -2.13685 | 5.00E-05 |
| Prom1 | chr5:44384860-44492975 | -1.807 | 5.00E-05 | -1.87344 | 5.00E-05 | -0.61318 | 1.00E-04 |
| Prtg | chr9:72655080-72765114 | -1.54327 | 5.00E-05 | -2.27627 | 5.00E-05 | -0.63292 | 5.00E-05 |
| Pvrl1 | chr9:43552658-43615544 | 0.526535 | 6.00E-04 | 0.546627 | 5.00E-04 | 0.584936 | 0.00025 |

| | | | | | | | |
|---|---|---|---|---|---|---|---|
| Rapgef3 | chr15:97575200-97598097 | 2.65567 | 5.00E-05 | 1.62714 | 5.00E-05 | 0.748318 | 5.00E-05 |
| Rem2 | chr14:55094936-55099271 | -1.54936 | 5.00E-05 | -1.91353 | 5.00E-05 | -1.22567 | 5.00E-05 |
| Robo4 | chr9:37209630-37221607 | 2.00539 | 5.00E-05 | 2.15718 | 5.00E-05 | 0.892419 | 0.0011 |
| Rpl21 | chr5:147644465-147648608 | 0.699351 | 5.00E-05 | 0.51325 | 0.0018 | 0.581381 | 0.00085 |
| Rpl24 | chr16:55966387-55971550 | 4.65949 | 5.00E-05 | 1.59877 | 5.00E-05 | 3.2531 | 2.00E-04 |
| Scg3 | chr9:75491172-75531863 | -2.85376 | 5.00E-05 | -1.16249 | 0.01035 | -1.02597 | 0.00055 |
| Sel1l3 | chr5:53498321-53604691 | -1.50661 | 5.00E-05 | -2.01273 | 5.00E-05 | -0.95405 | 5.00E-05 |
| Sema3c | chr5:17080633-17236085 | -4.30566 | 5.00E-05 | -3.94691 | 5.00E-05 | -1.20154 | 5.00E-05 |
| Sema3e | chr5:14025275-14256689 | -3.91725 | 5.00E-05 | -3.06641 | 5.00E-05 | -0.95584 | 5.00E-05 |
| Sema6a | chr18:47404907-47528522 | -4.44329 | 5.00E-05 | -2.70868 | 5.00E-05 | -0.66631 | 6.00E-04 |
| Sepp1 | chr15:3220766-3230508 | -2.12447 | 5.00E-05 | -2.23704 | 5.00E-05 | -0.6718 | 5.00E-05 |
| Sep-01 | chr7:134357955-134361959 | 2.33373 | 5.00E-05 | 2.52384 | 5.00E-05 | 0.586146 | 5.00E-05 |
| Serpinb9b | chr13:33119282-33132427 | -1.78457 | 5.00E-05 | -0.91234 | 5.00E-05 | -1.14882 | 0.00085 |
| Setbp1 | chr18:78947116-79306130 | -1.46674 | 5.00E-05 | -2.01701 | 5.00E-05 | -0.68813 | 0.00065 |
| Sfrp2 | chr3:83570242-83578236 | -2.17096 | 5.00E-05 | -3.06482 | 5.00E-05 | -0.50099 | 0.00095 |
| Sik1 | chr17:31981194-31992737 | 0.75926 | 5.00E-05 | 0.327054 | 0.02085 | 0.614043 | 5.00E-05 |
| Slc25a24 | chr3:108926066-108971327 | -1.66006 | 5.00E-05 | -1.74601 | 5.00E-05 | -0.64495 | 0.001 |
| Slc25a31 | chr3:40512792-40530016 | -0.741482 | 0.00105 | -0.58178 | 0.00825 | -0.79233 | 0.00125 |
| Slc39a8 | chr3:135488454-135551536 | -3.93631 | 5.00E-05 | -1.15251 | 5.00E-05 | -1.55514 | 5.00E-05 |
| Slc40a1 | chr1:45964914-45982439 | -1.52468 | 5.00E-05 | -1.80446 | 5.00E-05 | -0.60181 | 9.00E-04 |
| Slc6a7 | chr18:61155033-61173853 | 3.13082 | 5.00E-05 | 0.687493 | 2.00E-04 | 0.871278 | 0.0013 |
| Smad7 | chr18:75527018-75555588 | 0.573627 | 5.00E-05 | 1.3165 | 5.00E-05 | 0.707397 | 5.00E-05 |
| Sorbs2 | chr8:46593141-46913260 | -2.97706 | 5.00E-05 | -2.5608 | 5.00E-05 | -0.88513 | 5.00E-04 |
| St7 | chr6:17699215-17893022 | -1.26058 | 5.00E-05 | -0.62256 | 0.00875 | -0.74614 | 5.00E-04 |
| Stmn1 | chr4:134024234-134029758 | 0.720447 | 5.00E-05 | 0.4846 | 0.0011 | 0.566525 | 4.00E-04 |
| Tagln | chr9:45671773-45744141 | -6.90224 | 0.00025 | -7.9612 | 0.00025 | -1.12309 | 5.00E-04 |
| Tbx3 | chr5:120120677-120134610 | 1.07551 | 5.00E-05 | 1.61276 | 5.00E-05 | 0.904689 | 5.00E-05 |
| Tcl1 | chr12:106454964-106460947 | 2.48719 | 5.00E-05 | 1.86504 | 5.00E-05 | 0.51919 | 0.00025 |
| Tgfbi | chr13:56710963-56740700 | 2.28708 | 5.00E-05 | 0.700327 | 5.00E-05 | 0.793369 | 5.00E-05 |
| Tgm3 | chr2:129838109-129876135 | 0.670486 | 5.00E-05 | 1.77105 | 5.00E-05 | 0.762677 | 0.00085 |
| Thbs1 | chr2:117937657-117952869 | -4.61257 | 5.00E-05 | -6.2151 | 5.00E-05 | -1.49919 | 5.00E-05 |
| Tmcc3 | chr10:93977601-94053699 | -1.24245 | 5.00E-05 | -0.91384 | 5.00E-05 | -0.60138 | 0.001 |
| Tmem30b | chr12:74644100-74647382 | -0.566376 | 6.00E-04 | -0.53465 | 0.00115 | -0.57181 | 0.00115 |
| Tmem47 | chrX:78315982-78343214 | -2.77613 | 5.00E-05 | -1.16845 | 5.00E-05 | -0.65156 | 5.00E-05 |
| Tmprss2 | chr16:97786288-97832802 | -1.10488 | 5.00E-05 | -0.91877 | 0.00085 | -1.07183 | 0.00045 |
| Tns1 | chr1:73956804-74171021 | 1.15144 | 5.00E-05 | 0.48111 | 6.00E-04 | 0.76259 | 5.00E-05 |
| Tpm1 | chr9:66870399-66897020 | -2.17158 | 5.00E-05 | -2.77872 | 5.00E-05 | -0.59161 | 5.00E-05 |
| Tpm4 | chr8:74659190-74677028 | -0.58716 | 5.00E-05 | -0.76154 | 5.00E-05 | -0.50075 | 0.00025 |
| Tspan7 | chrX:10062241-10173730 | -0.960243 | 5.00E-05 | -0.8971 | 5.00E-05 | -0.53634 | 4.00E-04 |
| Unc45b | chr11:82724754-82778352 | -2.29703 | 5.00E-05 | -1.58203 | 5.00E-05 | -0.95523 | 5.00E-05 |
| Wls | chr3:159502658-159598139 | -0.590246 | 5.00E-04 | -1.7651 | 5.00E-05 | -0.71641 | 5.00E-05 |

| | | | | | | | |
|---|---|---|---|---|---|---|---|
| Zfp521 | chr18:13845522-14131242 | -1.08291 | 5.00E-05 | -0.80898 | 0.00115 | -0.68869 | 4.00E-04 |
| Zfp677 | chr17:21520711-21536229 | -1.53443 | 5.00E-05 | -2.64016 | 5.00E-05 | -0.81992 | 1.00E-04 |
| Zfp953 | chr13:67440244-67461508 | 0.413845 | 0.00695 | 1.87281 | 5.00E-05 | 0.579432 | 6.00E-04 |